

# Hessian-Aware Zeroth-Order Optimization for Black-Box Adversarial Attack

Haishan Ye \*    Zhichao Huang \*    Cong Fang †    Chris Junchi Li ‡    Tong Zhang \*

March 21, 2019

## Abstract

Zeroth-order optimization is an important research topic in machine learning. In recent years, it has become a key tool in black-box adversarial attack to neural network based image classifiers. However, existing zeroth-order optimization algorithms rarely extract second-order information of the model function. In this paper, we utilize the second-order information of the objective function and propose a novel *Hessian-aware zeroth-order algorithm* called **ZO-HessAware**. Our theoretical result shows that **ZO-HessAware** has an improved zeroth-order convergence rate and query complexity under structured Hessian approximation, where we propose a few approximation methods for estimating Hessian. Our empirical studies on the black-box adversarial attack problem validate that our algorithm can achieve improved success rates with a lower query complexity.

## Contents

<b>1</b>	<b>Introduction</b>	<b>2</b>
1.1	Main Contribution . . . . .	5
1.2	Related Work . . . . .	5
<b>2</b>	<b>Notation and Preliminaries</b>	<b>6</b>
2.1	Notation . . . . .	7
2.2	Properties of Smoothness and Convexity . . . . .	7
2.3	Gaussian Smoothing . . . . .	8
<b>3</b>	<b>Hessian-Aware Zeroth-Order Method</b>	<b>8</b>
3.1	Properties of Estimated Gradient . . . . .	9
3.2	Local Convergence . . . . .	10
3.3	Global Convergence . . . . .	10
3.4	Query Complexity Analysis . . . . .	11

---

\*Hong Kong University of Science and Technology; email: yhs12354123@gmail.com; zhuangbx@connect.ust.hk and tongzhang@tongzhang-ml.org

†Peking University; email: fangcong@pku.edu.cn

‡Tencent AI Lab; email: junchi.li.duke@gmail.com

<b>4</b>	<b>Structured Hessian Approximation</b>	<b>12</b>
4.1	Gaussian-Sampling Based Hessian Approximation . . . . .	12
4.2	Diagonalization Based Hessian Approximation . . . . .	13
<b>5</b>	<b>Experiments</b>	<b>14</b>
5.1	Algorithm Implementation . . . . .	15
5.1.1	Descent Checking . . . . .	16
5.2	Evaluation on MNIST . . . . .	16
5.3	Evaluation on ImageNet . . . . .	18
5.4	Discussion . . . . .	19
<b>6</b>	<b>Conclusion</b>	<b>20</b>
<b>A</b>	<b>Proof of Section 3.1</b>	<b>24</b>
A.1	Important Lemmas . . . . .	24
A.2	Proof of Lemma 1 . . . . .	24
A.3	Proof of Lemma 2 . . . . .	26
A.4	Proof of Lemma 3 . . . . .	27
<b>B</b>	<b>Proof of Convergence Rate of Algorithm 1</b>	<b>28</b>
B.1	Proof of Theorem 1 . . . . .	29
B.2	Proof of Theorem 2 . . . . .	35
<b>C</b>	<b>Proof of Section 3.4</b>	<b>37</b>
C.1	Proof of Theorem 3 . . . . .	37
C.2	Proof of Theorem 4 . . . . .	40
<b>D</b>	<b>Proof of Section 4</b>	<b>40</b>
D.1	Proof of Lemma 4 . . . . .	40
D.2	Proof of Lemma 5 . . . . .	41
<b>E</b>	<b>Parameter Setting</b>	<b>42</b>
<b>F</b>	<b>Visualization of Adversarial Attack</b>	<b>42</b>

# 1 Introduction

In this paper, we consider the following convex optimization problem:

$$\min_{x \in \mathbb{R}^d} f(x) \tag{1.1}$$

where  $f$  is differentiable and strongly convex. Optimization method that solves the above problem with function value access only is known as *zeroth-order optimization* or *black-box optimization* (Nesterov & Spokoiny, 2017; Ghadimi & Lan, 2013).

Zeroth-order optimization has attracted attention from the machine learning community (Bergstra et al., 2011; Ilyas et al., 2018) and it is especially useful for solving problem (1.1) where the evaluations of gradients  $\nabla f(x)$  are difficult or even infeasible. One prominent example of the zeroth-order optimization is the *black-box adversarial attack* on deep neural networks (Chen et al., 2017; Hu & Tan, 2017; Papernot et al., 2017; Ilyas et al., 2018). In the black-box adversarial attack, only the inputs and outputs of the neural network are available to the system and backpropagation on the target neural network is prohibited. Another application example is the hyper-parameter tuning which searches for the optimal parameters of deep neural networks or other learning models (Snoek et al., 2012; Bergstra et al., 2011).

In the past years, theoretical works on zeroth-order optimization arise as alternatives of the corresponding first-order methods, and they estimate gradients using function value difference (Nesterov & Spokoiny, 2017; Ghadimi & Lan, 2013; Duchi et al., 2015). However, these works on zeroth-order optimization have been concentrating on extracting gradient information of the objective function and *failed* to utilize the second-order Hessian information and, to some extent, have *not* fully exploited the information of models and enjoyed less competitive rates. In this paper, we aim to take advantages of the model’s second-order information and propose a novel method called *Hessian-aware* zeroth-order optimization. Aligning with earlier works Nesterov & Spokoiny (2017); Ghadimi & Lan (2013) we present in this paper our gradient estimation as follows:

$$g_\mu(x) = \frac{1}{b} \sum_{i=1}^b \frac{f(x + \mu \tilde{H}^{-1/2} u_i) - f(x)}{\mu} \cdot \tilde{H}^{1/2} u_i, \quad \text{with } \mu > 0 \quad (1.2)$$

where  $b$  is the batch size of points for gradient estimation and  $\tilde{H}$  is an approximate Hessian at the evaluation point. With Eqn. (1.2) at hands, the core update rule of our Hessian-aware zero-order algorithm, namely **Z0-HessAware**, is

$$x_{t+1} = x_t - \eta \tilde{H}^{-1} g_\mu(x_t) = x_t - \eta \tilde{H}^{-1} \cdot \frac{1}{b} \sum_{i=1}^b \frac{f(x + \mu \tilde{H}^{-1/2} u_i) - f(x)}{\mu} \cdot \tilde{H}^{1/2} u_i,$$

where  $\eta$  is the step size. If one lets  $\tilde{g}_\mu(x)$  be defined as

$$\tilde{g}_\mu(x) \triangleq \frac{1}{b} \sum_{i=1}^b \frac{f(x + \mu \tilde{u}_i) - f(x)}{\mu} \cdot \tilde{u}_i, \quad \text{with } \tilde{u}_i \sim N(0, \tilde{H}^{-1}), \quad (1.3)$$

then using the linear transformation property of the multivariate Gaussian distribution, the update rule further reduces to

$$x_{t+1} = x_t - \eta \tilde{g}_\mu(x_t). \quad (1.4)$$

In comparison, early zeroth-order literatures (for instance Nesterov & Spokoiny (2017)) conduct

gradient estimation via

$$\hat{g}_\mu(x) \triangleq \frac{1}{b} \sum_{i=1}^b \frac{f(x + \mu u_i) - f(x)}{\mu} u_i \quad \text{with } u_i \sim N(0, I_d). \quad (1.5)$$

We refer (1.5) as *vanilla zeroth-order optimization method*. Comparing (1.3) and (1.5), one observes that the directions of updates  $\tilde{g}_\mu$  and  $\hat{g}_\mu$  share the same form but admit different covariances. Because  $\tilde{g}_\mu(x)$  contains Hessian information and shares the same form with estimated gradient  $\hat{g}_\mu(x)$ ,  $\tilde{g}_\mu(x)$  can be regarded as a *natural gradient* and **Z0-HessAware** can be regarded as *natural gradient descent* method. Perhaps surprising, in the context of zeroth-order optimization the difference between our zeroth-order update and earlier works boil down to the difference of search direction covariances. Our special choice of covariance matrix as the approximate inversed Hessian allows us to incorporate Hessian information into the update rule in Eqn. (1.4), which further achieves an improved theoretical convergence rate in zeroth-order optimization.

Let the approximate Hessian  $\tilde{H}$  satisfy  $\rho\tilde{H} \preceq \nabla^2 f(x) \preceq (2-\rho)\tilde{H}$ , and  $\zeta \cdot I_d \preceq \tilde{H}$ , with  $0 < \rho \leq 1$  and  $\zeta > 0$ , and the algorithm be initialized at a point sufficiently close to the optimal solution. Our main result concludes that **Z0-HessAware** with a proper step size achieves an iteration complexity of  $N(\epsilon) = O\left(\frac{d}{b\rho} \log\left(\frac{1}{\epsilon}\right)\right)$ , in order to obtain an  $\epsilon$ -accuracy solution. If  $f(x)$  has the strong convexity parameter  $\tau$  and  $\rho$  is chosen as  $\tau/\lambda_{k+1}$  where  $\lambda_{k+1}$  upper-bounds the Hessian's  $(k+1)$ -th largest eigenvalue, then **Z0-HessAware** enjoys an iteration complexity (or convergence rate) of

$$N(\epsilon) = O\left(\frac{d\lambda_{k+1}}{b\tau} \log\left(\frac{1}{\epsilon}\right)\right).$$

Furthermore, let **Z0-HessAware** be implemented with power-method based Hessian approximation (namely **ZOHA-PW**) (Balcan et al., 2016), it achieves the following query complexity

$$Q(\epsilon) = \tilde{O}\left(\frac{dk\lambda_{k+1}}{\tau} \log\left(\frac{1}{\epsilon}\right)\right).$$

Let  $L$  be the smoothness parameter of the objective function, vanilla zeroth-order optimization method (Nesterov & Spokoiny, 2017) shows an iteration complexity of  $O\left(\frac{dL}{b\tau} \log\left(\frac{1}{\epsilon}\right)\right)$  and a query complexity of  $O\left(\frac{dL}{\tau} \log\left(\frac{1}{\epsilon}\right)\right)$ . Under a low-rank Hessian structure that  $k\lambda_{k+1} \leq L$ , our proposed **Z0-HessAware** algorithm enjoys a sharper theoretical convergence rate and query complexity than vanilla zeroth-order method (1.5).

Though **ZOHA-PW** obtains a nice theoretical result of query complexity, it takes at least  $O(d)$  queries due to the power method procedure. This is very expensive especially when the dimension  $d$  is very large. Hence, we also propose two heuristic but practical methods to construct approximate Hessians with much lower query complexity.

- (i) First, we use Gaussian sampling method to approximate Hessian. This method only samples a small batch of points from the Gaussian distribution to estimate the Hessian with batch size being much smaller than the data dimension  $d$ .

- (ii) Second, we propose diagonal Hessian approximation which is a popular method in training deep neural networks. This approximation approach does not need extra query to function value and can keep principal information of the Hessian which has been proved in training deep neural networks (Kingma & Ba, 2015; Duchi et al., 2011; Zeiler, 2012).

To numerically justify the effectiveness of our zeroth-order algorithm **ZO-HessAware**, we apply it to the task of black-box adversarial attack in the neural network based image classifier (Ilyas et al., 2018; Chen et al., 2017). The adversarial attack aims to find an example  $x$  deviated microscopically from the given image  $x_0$  but misclassified by the neural network classifier. We compare our algorithms with two state-of-the-arts, namely PGD-NES (Ilyas et al., 2018) and ZOO (Chen et al., 2017). The comparison shows that our two **ZO-HessAware** algorithm variants take reduced function value queries while obtaining an improved success rate of attack and exhibits outstanding performance especially when the attack task is hard. Furthermore to promote the attack success rate and reduce the query complexity, we propose a novel strategy call **Descent-Checking** which empirically brings an even higher success rate and lower query complexity.

## 1.1 Main Contribution

We summarize our main contribution as follows.

- (i) We exploit the Hessian information of the model function and propose a novel Hessian-aware zeroth-order algorithm called **ZO-HessAware**. We integrate Hessian information into gradient estimation while keeping the algorithmic form similar to vanilla zeroth-order method. Theoretically we show **ZO-HessAware** has a faster convergence rate and lower query complexity with power-method based Hessian approximation than existing work without Hessian information.
- (ii) Several novel structured Hessian approximation methods are proposed including Gauss sampling method as well as the diagonalization method. The Hessian estimation via Gauss sampling only takes a few extra queries to the function value. In the construction of diagonal approximate Hessian, we use natural gradient which contains Hessian information other than an ordinary gradient which is used in training deep neural networks.
- (iii) We propose a descent-checking trick for the black-box adversarial attack. This trick can significantly improve the success rate and reduce the number of queries.
- (iv) We empirically prove the power of Hessian information in zeroth-order optimization especially in the black-box adversarial attack. Experiment results show that our **ZO-HessAware** type algorithm can achieve better success rates and need fewer queries than state-of-the-art algorithms especially when the problem is hard.

## 1.2 Related Work

Zeroth-order optimization minimizes functions only through the function value oracles. It is an important research topic in optimization (Nesterov & Spokoiny, 2017; Matyas, 1965; Ghadimi & Lan, 2013). Nesterov & Spokoiny (2017) utilized random Gaussian vectors as the search directions

and gave the convergence properties of the zeroth-order algorithms when the objective function is convex. Ghadimi & Lan (2013) proposed new zeroth-order algorithms which has better convergence rate when the problem is non-smooth. Zeroth-order method with variance reduction was proposed to solve non-convex problem recently (Fang et al., 2018; Liu et al., 2018). Zeroth-order algorithm is also a crucial research topic in the on-line learning. Lots of results were obtained in the recent years (Shamir, 2017; Bach & Perchet, 2016; Duchi et al., 2015). In these works, one can only access to the function value and uses this feed-back to approximate the gradient or sub-gradient.

Recently, zeroth-order algorithm is becoming the main tool for the black-box adversarial attack (Chen et al., 2017; Ilyas et al., 2018). Chen et al. (2017) extended the CW (Carlini & Wagner, 2017) attack which is a powerful white-box method to the black-box attack and proposed ZOO. Algorithm ZOO can be viewed as a kind of zeroth-order stochastic coordinate descent (Chen et al., 2017). It chooses a coordinate randomly, then uses zeroth-order oracles to estimate the gradient of current coordinate. However, ZOO suffers from a poor query complexity because it needs  $O(d)$  queries to estimate the gradients of all the coordinates theoretically. To reduce the query complexity, Ilyas et al. (2018) resorted to the natural evolutionary strategies (Wierstra et al., 2014) to estimate gradients. And Ilyas et al. (2018) used the so-called ‘antithetic sampling’ technique (Salimans et al., 2017) to get better performance.

Furthermore, covariance matrix adaptation evolution strategy (CMA-ES) is another important zeroth-order method which is closely related to our algorithm (Hansen & Ostermeier, 2001). CMA-ES uses a learned covariance to generate search direction and this covariance matrix is much like the inversion of our approximate Hessian. The main difference between these two algorithms is the way to use zeroth-order oracles. Eqn. (1.3) shows that ZO-HessAware queries to function value to approximate a natural gradient. In contrast, CMA-ES generates  $u_i$ ’s and picks up such  $\tilde{u}_i$ ’s as the search directions that  $f(x + \tilde{u}_i)$  is small.

**Organization.** The rest of this paper is organized as follows. In Section 2, we present notation and preliminaries. In Section 3, we depict Algorithm ZO-HessAware in detail and analyze its local and global convergence rate, and query complexity with power-method based Hessian approximation, respectively. In Section 4, we propose two different strategies to construct a good approximate Hessian. In Section 5, we compare our ZO-HessAware type algorithms with two state-of-the-art algorithms in the adversarial attack problem. Finally, we conclude our work in Section 6. All the detailed proofs are deferred to the appendix in their order of appearance.

## 2 Notation and Preliminaries

We first introduce notation that will be used in this paper. Then, we give some assumptions about the objective function that will be used.

## 2.1 Notation

Given a positive semi-definite matrix  $A \in \mathbb{R}^{d \times d}$  of rank- $\ell$  and a positive integer  $k \leq \ell$ , its eigenvalue decomposition is given as

$$A = U\Lambda U^T = U_k \Lambda_k U_k^T + U_{\setminus k} \Lambda_{\setminus k} U_{\setminus k}^T, \quad (2.1)$$

where  $U_k$  and  $U_{\setminus k}$  contain the eigenvectors of  $A$ , and  $\Lambda = \text{diag}(\lambda_1, \dots, \lambda_d)$  with  $\lambda_1 \geq \lambda_2 \geq \dots \geq \lambda_\ell > 0$  are the nonzero eigenvalues of  $A$ . We also use  $\lambda_{\max}$  and  $\lambda_{\min}$  to denote the largest and smallest eigenvalue of a positive semi-definite matrix, respectively.

Using matrix  $A$ , we can define  $A$ -norm as  $\|x\|_A = \sqrt{x^T A x}$ . Furthermore, if  $B$  is a positive semi-definite matrix, we say  $B \preceq A$  when  $A - B$  is positive semi-definite.

## 2.2 Properties of Smoothness and Convexity

In this paper, we consider functions with  $L$ -smoothness and  $\tau$ -strongly convexity. It indicates the following properties.

**$L$ -smoothness** Let function  $f(x)$  be  $L$ -smooth, i.e. for all  $x, y \in \mathbb{R}^d$ , we have

$$\|\nabla f(x) - \nabla f(y)\| \leq L \|x - y\|, \quad (2.2)$$

or equivalently

$$|f(y) - f(x) - \langle \nabla f(x), y - x \rangle| \leq \frac{L}{2} \|x - y\|^2. \quad (2.3)$$

**$\tau$ -strong convexity** Let function  $f(x)$  be  $\tau$ -strongly convex, i.e. for all  $x, y \in \mathbb{R}^d$

$$f(y) \geq f(x) + \langle \nabla f(x), y - x \rangle + \frac{\tau}{2} \|x - y\|^2.$$

**$\gamma$ -Lipschitz Hessian** Let the Hessian of  $f(x)$  be  $\gamma$ -Lipschitz continuous, that is, for all  $x, y \in \mathbb{R}^d$

$$\|\nabla^2 f(y) - \nabla^2 f(x)\| \leq \gamma \|y - x\|. \quad (2.4)$$

or equivalently

$$\left| f(y) - f(x) - \langle \nabla f(x), y - x \rangle - \frac{1}{2} \langle \nabla^2 f(x)(y - x), y - x \rangle \right| \leq \frac{\gamma}{6} \|x - y\|^3, \quad x, y \in \mathbb{R}^d \quad (2.5)$$

### 2.3 Gaussian Smoothing

Let  $f(x)$  be a function which is differentiable along any direction in  $\mathbb{R}^d$ . The *Gaussian smoothing* of  $f(x)$  is defined as

$$f_\mu(x) \triangleq \frac{1}{M} \int_{\mathbb{R}^d} f(x + \mu u) \exp\left(-\frac{\|u\|^2}{2}\right) du, \text{ where } u \sim N(0, I_d), \quad (2.6)$$

and

$$M = \int_{\mathbb{R}^d} \exp\left(-\frac{\|u\|^2}{2}\right) du = (2\pi)^{d/2}.$$

And  $\mu$  is the parameter to control the smoothness.  $f_\mu(x)$  preserves several important properties of  $f(x)$ . For example, if  $f(x)$  is convex, then  $f_\mu(x)$  is also convex. If  $f(x)$  is  $L$ -smooth, then  $f_\mu(x)$  is also  $L$ -smooth.

## 3 Hessian-Aware Zeroth-Order Method

In this section, we will exploit the Hessian information of the model function which was commonly ignored in the past works on zeroth-order optimization and propose **ZO-HessAware** algorithm.

Our algorithm first constructs an approximate Hessian  $\tilde{H}$  for the current point  $x$  satisfies

$$\rho\tilde{H} \preceq \nabla^2 f(x) \preceq (2 - \rho) \cdot \tilde{H}, \text{ and, } \zeta \cdot I_d \preceq \tilde{H}, \quad (3.1)$$

with  $0 < \rho \leq 1$ . Parameter  $\rho$  measures how well  $\tilde{H}$  approximates  $\nabla^2 f(x)$ . If  $\rho = 1$ , then  $\tilde{H}$  is the exact Hessian. One can use different methods to construct such  $\tilde{H}$ . In Section 4, we will provide several approaches to compute a good approximate Hessian with a small number of queries to the function value. Note that, we do not need to construct an approximate Hessian for each iteration. Empirically, we can only update it every  $p$  iterations where  $p$  is a parameter controls the frequency of the Hessian approximation.

Then we begin to estimate the gradient by derivative-free oracles. Different from the existing zeroth-order works (Nesterov & Spokoiny, 2017; Ghadimi & Lan, 2013; Duchi et al., 2015), the Hessian information is used in our gradient estimation represented as follows:

$$g_\mu(x) = \frac{1}{b} \sum_{i=1}^b \frac{f(x + \mu K u_i) - f(x)}{\mu} K^{-1} u_i, \text{ with } K = \tilde{H}^{-1/2}, u_i \sim N(0, I) \quad (3.2)$$

where  $b$  is the batch size. On the point  $x$ , we sample  $b + 1$  points to obtain a good gradient estimation. This strategy is widely used in real applications such as adversarial attack.

Finally, analogue to Newton-style algorithms, we update  $x_{t+1}$  using the approximate Hessian and estimated gradient as  $x_{t+1} = x_t - \eta \tilde{H}^{-1} g_\mu(x)$ . Combining with Eqn. (3.2), we represent the



---

**Algorithm 1** Algorithm Z0-HessAware
 

---

- 1: **Input:**  $x^{(0)}$  is an initial point sufficient close to  $x^*$ . And  $b$  is the batch size and  $p$  is an integer. Parameter  $\eta$  is the step size.
  - 2: **for**  $t = 0, \dots, T$  **do**
  - 3:   **if**  $t \bmod p == 0$  **then**
  - 4:     Compute an approximate Hessian  $\tilde{H}_t$  satisfies Eqn. (3.1).
  - 5:   **end if**
  - 6:   Generate  $b$  samples with  $u_i \sim N(0, I_d)$  and construct  $\tilde{g}_\mu(x_t) = \frac{1}{b} \sum_{i=1}^b \frac{f(x + \tilde{H}_t^{-1/2} u_i) - f(x)}{\mu} \tilde{H}_t^{-1/2} u_i$ ;
  - 7:   Update  $x_{t+1} = x_t - \eta \tilde{g}_\mu(x_t)$ .
  - 8: **end for**
- 

algorithmic procedure of Z0-HessAware as follows

$$\begin{cases} \tilde{g}_\mu(x_t) = \frac{1}{b} \sum_{i=1}^b \frac{f(x_t + \mu \tilde{H}_t^{-1/2} u_i) - f(x_t)}{\mu} \tilde{H}_t^{-1/2} u_i, \text{ with } u_i \sim N(0, I) \\ x_{t+1} = x_t - \eta \tilde{g}_\mu(x_t). \end{cases}$$

We depict the detailed algorithmic procedure of Z0-HessAware in Algorithm 1.

In the rest of this section, we will first give some important properties of the estimated gradient computed as Eqn. (3.2). Then we analyze the local and global convergence property of Algorithm 1, respectively. Finally, the query complexity will be analyzed with power-method based Hessian approximation.

### 3.1 Properties of Estimated Gradient

Now, we list some important properties of  $g_\mu(x)$  defined in Eqn. (3.2) that will be used in our analysis of convergence rate of Z0-HessAware in the following lemmas. These lemmas are also of independent interest in zeroth-order algorithm.

**Lemma 1.** *Let  $f(x)$  be  $L$ -smooth, then  $g_\mu(x)$  defined in Eqn. (3.2) satisfies that*

$$\|\mathbb{E}_u[g_\mu(x)] - \nabla f(x)\|_{K^2}^2 \leq \frac{\mu^2}{4} L^2 \|K\|^4 (d+3)^3.$$

**Lemma 2.** *Let  $f(x)$  be  $L$ -smooth, then  $\|g_\mu(x)\|_{K^2}^2$  can be bounded as*

$$\mathbb{E}_u \|g_\mu(x)\|_{K^2}^2 \leq \frac{\mu^2}{2b} L^2 \|K\|^4 (d+6)^3 + \left( \frac{2(d+2)}{b} + 2 \right) \cdot \|\nabla f(x)\|_{K^2}^2 + \frac{\mu^2 L^2 (d+3)^3}{2}.$$

Now we give the bound of  $\mathbb{E}_u \|K^2 g_\mu(x)\|_{K^{-2}}^3$  in the following lemma.

**Lemma 3.** *Let  $f(x)$  be  $L$ -smooth, then  $g_\mu(x)$  has such a property that*

$$\mathbb{E}_u \|K^2 g_\mu(x)\|_{K^{-2}}^3 \leq 2\mu^3 L^3 \|K\|^6 \cdot (d+9)^{9/2} + 12(d+5)^{3/2} \|\nabla f(x)\|_{K^2}^3.$$

### 3.2 Local Convergence

Now we begin to analyze the local convergence property of Algorithm 1. To achieve a fast convergence rate, the initial point should be close enough to the optimal point. At the same time, the Hessian should be well-approximated.

**Theorem 1.** *Let  $f(x)$  be  $\tau$ -strongly convex and  $L$ -smooth, and  $\nabla^2 f(x)$  is  $\gamma$ -Lipschitz continuous. Let the approximate Hessian  $\tilde{H}_t$  satisfy Eqn. (3.1). Setting the step size  $\eta = \frac{b}{16(d+2)}$  and  $b \leq d+2$ , then Algorithm 1 has the following convergence properties:*

$$\mathbb{E}[f(x_{t+1}) - f(x^*)] \leq \left(1 - \frac{b\rho}{64(d+2)}\right) (f(x_t) - f(x^*)) + \Delta_\mu,$$

if  $x_t$  satisfies that

$$\|x_t - x^*\| \leq \frac{\rho}{\gamma} \cdot \min\left(\frac{3\tau\zeta^{1/2}}{64L^{1/2}}, \frac{d^{3/2}\zeta^2}{33L(d+2)b^2}\right), \quad (3.3)$$

and  $\Delta_\mu$  is defined as

$$\Delta_\mu = b \cdot \left(\frac{\mu^2 L^2}{64\zeta^2}(d+5)^2 + \frac{\mu^2 L^2}{128\zeta}(d+38) + \frac{\gamma b^2 \mu^3 L^3}{6144\zeta^{9/2}} \cdot (d+110)^{3/2}\right).$$

**Remark 1.** *Note that, the local convergence properties rely on the condition (3.3). However, this condition may be violated for next iteration if the descent direction is not good. This problem can be remedied by checking the value of  $f(x_{t+1})$ . We will discard the current  $x_{t+1}$  if  $f(x_{t+1})$  is larger than  $f(x_t)$ .*

Let  $\rho$  be chosen  $O(\tau/\lambda_{k+1})$ , then to achieve an  $\epsilon$ -accuracy solution, by Theorem 1, our Z0-HessAware needs

$$N(\epsilon) = O\left(\frac{d}{b\rho} \log\left(\frac{1}{\epsilon}\right)\right) = O\left(\frac{d\lambda_{k+1}}{b\tau} \log\left(\frac{1}{\epsilon}\right)\right)$$

iterations. In contrast, without the second-order information, vanilla zeroth-order method needs  $O(db^{-1}\kappa \log(\frac{1}{\epsilon}))$  iterations (Nesterov & Spokoiny, 2017), where  $\kappa = L/\tau$  is the condition number. Since it holds that  $\lambda_{k+1} \leq L$ , Z0-HessAware has a faster convergence rate. Especially when the Hessian can be well approximated by a rank- $k$  matrix, that is  $\lambda_{k+1} \ll L$ , our algorithm will show great advantages.

### 3.3 Global Convergence

We will analyze the global convergence property of Algorithm 1 in this section. To guarantee a global convergence, we have to set a smaller step size compared with the one set in Theorem 1. Then, we have the following theorem.

---

**Algorithm 2** Power-method Based Hessian Approximation.

---

- 1: **Input:** Orthonormal matrix  $V_0 \in \mathbb{R}^{d \times k}$  where  $k$  is the target rank;
  - 2: **for**  $t = 0, \dots, T - 1$  **do**
  - 3:   Approximate the  $\nabla^2 f(x)V_t$  by  $Y_t = H_\mu V_t$  implemented as Eqn. (3.4);
  - 4:   QR factorization:  $Y_t = V_{t+1}R_{t+1}$ , where  $V_{t+1}$  consists of orthonormal columns.
  - 5: **end for**
  - 6: Compute  $Y = H_\mu V_T$  and compute the SVD decomposition  $Y = \hat{U}\Lambda\hat{V}^\top$ .
  - 7: **Return:**  $\tilde{H} = V\Lambda V^\top + 5\lambda_{k+1}I_d$  with  $V = V_T\hat{V}$
- 

**Theorem 2.** *Let function  $f(x)$  satisfy the properties described in Theorem 1. For each iteration, the approximate Hessian  $\tilde{H}_t$  satisfies Eqn. (3.1). By choosing the step size  $\eta = \frac{\zeta}{4(d+2)L}$ , Algorithm 1 has the following convergence property*

$$\mathbb{E}_u [f(x_{t+1}) - f(x^*)] \leq \left(1 - \frac{b\zeta}{16(d+2)\kappa L}\right) \cdot (f(x_t) - f(x^*)) + \Delta_\mu,$$

where  $\Delta_\mu$  is defined as

$$\Delta_\mu = \frac{b\mu^2 L}{64\zeta(d+2)} \left(2(d+3)^3 + \frac{(d+6)^3}{d+2}\right).$$

In our analysis of global convergence, we set a fixed step size. We can also use the line search method to get a better convergence property at the cost of extra query to the function value.

### 3.4 Query Complexity Analysis

In this section, we will analyze the query complexity of ZOHA-PW which implements ZO-HessAware with power-method based Hessian approximation. The power method only needs to access Hessian-Vector product which can be approximated by

$$[\nabla^2 f(x)v]_i \approx [H_\mu v]_i \triangleq \frac{f(x + \mu_1 \cdot (v + e_i)) - f(x + \mu_1 \cdot (v - e_i)) + f(x - \mu_1 \cdot e_i) - f(x + \mu_1 \cdot e_i)}{2\mu_1^2}, \quad (3.4)$$

where  $[H_\mu v]_i$  means the  $i$ -th entry of vector  $H_\mu v$ . Note that,  $H_\mu$  does not need to be explicitly represented. And it can be regarded as the Hessian  $\nabla^2 f(x)$  with some small perturbations.

Given the above results to approximating Hessian-vector product, we conduct power method to obtain the  $k$ -largest eigenvalue and their corresponding eigenvectors. The detailed algorithmic procedure is depicted in Algorithm 2. Then the approximate Hessian  $\tilde{H}$  computed based on power method has the following properties.

**Theorem 3.** *Let the objective function satisfy Eqn. (2.4). Let  $\mu_1$  and the iteration number  $T$  satisfy that*

$$\mu_1 \leq \min \left\{ \frac{C_1}{4k\gamma} \lambda_{k+1}, \frac{C_2}{4} \cos(U_k, V_0) \right\} \text{ and } T = 2C_3 \log(2 \tan(U_k, V_0))$$

where  $U_k$  is the matrix consists of eigenvectors corresponding to the first  $k$  largest eigenvalues of

$\nabla^2 f(x)$ .  $C_1$ ,  $C_2$ , and  $C_3$  are absolute constants. Then  $\tilde{H}$  returned from Algorithm 2 has the following property

$$\frac{\lambda_{\min}}{\lambda_{\min} + 10\lambda_{k+1}} \tilde{H} \preceq \nabla^2 f(x) \preceq \tilde{H}, \text{ and, } 5\lambda_{k+1}I_d \preceq \tilde{H}.$$

The definition of the angle between two spaces  $U_k$  and  $V_0$  can be found in the textbook (?). Theorem 3 provides a specific choice of  $\rho = \frac{\lambda_{\min}}{\lambda_{\min} + 10\lambda_{k+1}}$  in Eqn. (3.1). Combining the convergence rate in Theorem 1, we give the query complexity analysis of ZOHA-PW which implements ZO-HessAware with power-method based Hessian approximation (Balcan et al., 2016).

**Theorem 4.** *Set the  $b = O(d)$  and  $p = 1$  in Algorithm 1. Then the query complexity of ZOHA-PW is*

$$Q(\epsilon) = \tilde{O} \left( \frac{dk\lambda_{k+1}}{\tau} \cdot \log \left( \frac{1}{\epsilon} \right) \right).$$

The approximate Hessian  $\tilde{H}$  constructed using power method can capture the dominant rank- $k$  information of  $\nabla^2 f(x)$ . We have the empirical fact that the Hessian of model function can be represented as a rank- $k$  matrix containing the dominant information, plus a perturbation matrix of small spectral norm (Yuan et al., 2007; Bakker et al., 2018; Sainath et al., 2013). In the case that  $k \cdot \lambda_{k+1} < L$ , the query complexity of ZOHA-PW is smaller than vanilla zeroth-order methods without Hessian information which takes  $O\left(\frac{dL}{\tau} \cdot \log\left(\frac{1}{\epsilon}\right)\right)$  queries shown in the work of Nesterov & Spokoiny (2017). If the Hessian update frequency  $p > 1$ , then the query complexity of ZOHA-PW can further be reduced.

Furthermore, we can use  $V_T$  of the last iteration of Algorithm 1 as the input  $V_0$  of Algorithm 2. Because  $x_t$  is close to the optimal point  $x^*$ , the value of  $\tan(U_k, V_0)$  can be regarded as a constant, that is, we can obtain an approximate Hessian in  $O(dk)$  query complexity. Hence, the query complexity of ZOHA-PW can be further improved to  $O\left(\frac{dk\lambda_{k+1}}{\tau} \cdot \log\left(\frac{1}{\epsilon}\right)\right)$ .

## 4 Structured Hessian Approximation

In this section, we will provide two kinds of *heuristic* methods to construct approximate Hessian. These methods takes much fewer queries to function value compared with power-method based Hessian approximation which takes at least  $O(dk)$  queries. The first method is based on Gauss sampling and the second one is based on diagonalization.

### 4.1 Gaussian-Sampling Based Hessian Approximation

We propose a novel method to approximate the Hessian of  $f(x)$  with a much lower query complexity than power method. It is based on Gaussian Sampling, and we name ZO-HessAware implemented with such Hessian approximation as ZOHA-Gauss.

Our new method is going to estimate the Hessian of  $f_\mu(x)$  defined in Eqn. (2.6). Since  $\nabla^2 f_\mu(x)$  is close to  $\nabla^2 f(x)$  if  $\mu$  is small, a good approximation of  $\nabla^2 f_\mu(x)$  will also approximate  $\nabla^2 f(x)$  well. In fact, we can bound the error between  $\nabla^2 f(x)$  and  $\nabla^2 f_\mu(x)$  as follows.

**Lemma 4.** Let  $f_\mu(x)$  be defined in Eqn. (2.6). The objective function  $f(x)$  satisfies Eqn. (2.4). Then, we have

$$\|\nabla^2 f_\mu(x) - \nabla^2 f(x)\| \leq \gamma\mu(d+1)^{1/2}.$$

Using Gaussian sampling, we can approximate the Hessian of  $f_\mu(x)$  as follows:

$$\tilde{H} = b^{-1} \sum_{i=1}^b \frac{f(x + \mu u_i) + f(x - \mu u_i) - 2f(x)}{2\mu^2} u_i u_i^\top + \lambda I_d, \text{ with } u_i \sim N(0, I_d) \quad (4.1)$$

where  $\lambda$  is a properly chosen regularizer to keep  $\tilde{H}$  invertible. In the construction of  $\tilde{H}$  of Eqn. (4.1), we only take a small batch of points, that is  $b$  is small even much smaller the dimension  $d$ . Hence, the construction of such  $\tilde{H}$  has a low query complexity.

The approximate Hessian  $\tilde{H}$  constructed as Eqn. (4.1) has the following property.

**Lemma 5.** Let  $\tilde{H}$  be an approximate Hessian defined in Eqn. (4.1). Function  $f_\mu(x)$  is the smoothed function defined in Eqn. (2.6). Then  $\tilde{H}$  has the following property

$$\nabla^2 f_\mu(x) \preceq \mathbb{E}_u[\tilde{H}] = \nabla^2 f_\mu(x) + \left( \lambda - \frac{f(x) - f_\mu(x)}{\mu^2} \right) \cdot I_d$$

Combining Lemma 4 and 5, we can obtain the result that if  $\mu$  is small, and the batch size  $b$  in Eqn. 4.1 is large, then  $\tilde{H}$  constructed as Eqn. (4.1) can approximate  $\nabla^2 f(x)$  well. In practice, we prefer to choosing a small batch size  $b$  to achieve query efficiency.

## 4.2 Diagonalization Based Hessian Approximation

We propose to use a diagonal matrix to approximate the Hessian. This method has been used in the optimization of deep neural networks (Kingma & Ba, 2015; Zeiler, 2012; Tieleman & Hinton, 2012) and online learning (Duchi et al., 2011).

First, we compute an approximate Hessian in the manner of ADAM (Kingma & Ba, 2015) as follows:

$$\begin{aligned} \tilde{g}_\mu(x_{t-1}) &= \frac{1}{b} \sum_{i=1}^b \frac{f(x_{t-1} + \mu \tilde{u}_i) - f(x_{t-1})}{\mu} \tilde{u}_i, \text{ with } \tilde{u}_i \sim N(0, \tilde{H}_{t-1}^{-1}) \\ D_t &= \nu D_{t-1} + (1 - \nu) \tilde{g}_\mu^2(x_{t-1}) \\ \tilde{H}_t &= \text{diag} \left( \frac{D_t}{1 - \nu^t} \right) \end{aligned} \quad (4.2)$$

with  $0 \leq \nu \leq 1$ . And  $\tilde{g}_\mu^2(x)$  means the entry-wise square of  $\tilde{g}_\mu(x)$ .

Second, we can also use the method of ADAGRAD (Duchi et al., 2011) to construct the approximate

Hessian as

$$\begin{aligned}\tilde{g}_\mu(x_{t-1}) &= \frac{1}{b} \sum_{i=1}^b \frac{f(x_{t-1} + \mu \tilde{u}_i) - f(x_{t-1})}{\mu} \tilde{u}_i, \text{ with } \tilde{u}_i \sim N(0, \tilde{H}_{t-1}^{-1}) \\ D_t &= D_{t-1} + \tilde{g}_\mu^2(x_{t-1}) \\ \tilde{H}_t &= \text{diag} \left( \frac{D_t}{n} \right).\end{aligned}$$

Other methods of constructing diagonal Hessian approximation such as ADADELTA (Zeiler, 2012) used in training deep neural networks can also be use to in our diagonal Hessian approximation.

These kinds of Hessian approximation are heuristic. We can not give an exact convergence rate of ZO-HessAware with diagonal Hessian approximation by Theorem 1. However, diagonal Hessian approximations have shown their power in training deep neural networks. Furthermore, diagonal approximate Hessian has an important advantage that it does not need extra queries to the function value and need less computational and storage cost.

Though the construction procedure of the diagonal Hessian approximation is the same with the one of ADAM and ADAGRAD, there some difference between these diagonal Hessians. First, ADAM and ADAGRAD use  $\tilde{H}^{1/2}$  as the approximate Hessian in training neural network which is different from our approximate Hessian. Second, in the construction of our diagonal Hessian, we use the ‘natural gradient’ defined in Eqn. (1.3) which contains the Hessian information other than the ordinary gradient. And the information of the current diagonal Hessian will be used in the estimation of next ‘natural gradient’. In contrast, the diagonal Hessian will not affect the computation of gradients.

## 5 Experiments

In this section, we apply our Hessian-aware zeroth-order algorithm to the black-box adversarial attacks. This is an important research topic in security of deep learning because neural networks are widely used in image classification. However, current neural network-based classifiers are susceptible to adversarial examples.

Our adversarial attack experiments include both targeted attack and un-targeted attack. The targeted attack aims to find an adversarial example  $x$  of a given image  $x_0$  with a targeted class label  $\ell$  toward misclassification. In this case, we are going to minimize the following problem proposed in the work of Carlini & Wagner (2017):

$$f(x, \ell) = \max \left\{ \max_{i \neq \ell} \log[Z(x)]_i - \log[Z(x)]_\ell, -\omega \right\}, \quad (5.1)$$

with constraint that

$$\|x - x_0\|_\infty \leq \varepsilon. \quad (5.2)$$

$Z(x)$  is the logit layer representation after softmax in the DNN for  $x$  such that  $[Z(x)]_i$  represents the predicted probability that  $x$  belongs to class  $i$ .  $\omega$  is a tuning parameter for attack transferability

and we set  $\omega = 1$  in our experiments. The constraint means that the adversarial image should be close to the given image.

The un-targeted adversarial attack aims to find an example  $x$  of the given image  $x_0$  with label  $\ell$  but misclassified by the neural network. In this case, we will minimize the following function (Carlini & Wagner, 2017) with constraint (5.2):

$$f(x) = \max \left\{ \log[Z(x)]_\ell - \max_{i \neq \ell} \log[Z(x)]_i, -\omega \right\}. \quad (5.3)$$

## 5.1 Algorithm Implementation

In the experiments, we will implement **ZO-HessAware** (Algorithm 1) with two different kinds of Hessian approximation. The first one is based on the Gaussian sampling described in Section 4.1, and we call it **ZOHA-Gauss**. The second implementation is using the diagonal Hessian approximation described in Section 4.2 with the update procedure as **ADAM** defined in Eqn. (4.2). And we name it as **ZOHA-Diag**. We do not implement **ZO-HessAware** with other kinds of diagonal Hessian approximation because these methods have the similar performance.

Furthermore, because the adversarial problem is of constraint, we will modify the update step (7) of Algorithm 1 as follows:

$$x_{t+1} = \Pi[x_t - \eta \tilde{g}_\mu(x_t)], \quad (5.4)$$

where  $\Pi[\cdot]$  is a projection operator to make  $x_{t+1}$  satisfy  $\|x_{t+1} - x_0\|_\infty \leq \epsilon$ . Note that, this projection is exact for **ZOHA-Diag**. But as to **ZOHA-Gauss**, we should compute  $x_{t+1}$  by optimizing the following sub-problem:

$$x_{t+1} = \underset{y \in [x_0 - \epsilon, x_0 + \epsilon]}{\operatorname{argmin}} \left\| y - \left( x_t - \eta \tilde{H}_t^{-1} g_\mu(x_t) \right) \right\|_{\tilde{H}}^2. \quad (5.5)$$

However, the projection as Eqn. (5.4) performs well and is of simple implementation even it is just an approximation to the true one computed by Eqn. (5.5).

Because the objective function of the neural network model may be non-convex, we implement the approximate Hessian in **ZOHA-Gauss** as follows:

$$\tilde{H} = b^{-1} \sum_{i=1}^b \frac{|f(x + \mu u_i) + f(x - \mu u_i) - 2f(x)|}{2\mu^2} u_i u_i^\top + \lambda I_d, \text{ with } u_i \sim N(0, I_d).$$

Such modification ensures that such  $\tilde{H}$  is positive definite. Furthermore, we observe that  $\tilde{H}$  can be written as  $\tilde{H} = CC^\top + \lambda I$ . Then we can compute  $\tilde{H}^{-1/2}$  as follows. First, we compute the SVD decomposition of  $C$  as  $C = U_C \Lambda_C U_C^\top$  with  $U_C \in \mathbb{R}^{d \times b}$  and  $\Lambda_C \in \mathbb{R}^{b \times b}$ . And we get  $\tilde{H}^{-1/2} = U_C ((\Lambda_C^2 + \lambda I)^{-1/2} - \lambda^{-1/2} I) U_C^\top + \lambda^{-1/2} I$ . In practice, the value of  $\lambda$  can be set as a fraction of  $\|CC^\top\|$  or tuned by several tries.

---

**Algorithm 3** Algorithm ZO-HessAware with descent checking (ZOHA-DC)

---

- 1: **Input:**  $x^{(0)}$  is an initial point sufficient close to  $x^*$ . And  $b$  is the batch size and  $p$  is an integer. Parameter  $\eta$  is the step size.  $\beta$  is the threshold of sample size in descent checking.  $\delta_b$  is the parameter of the sample size increment.
  - 2: **for**  $t = 0, \dots, T$  **do**
  - 3:   **if**  $t \bmod p == 0$  **then**
  - 4:     Compute an approximate Hessian  $\tilde{H}_t$  satisfies Eqn. (3.1).
  - 5:   **end if**
  - 6:   Generate  $b$  samples with  $u_i \sim N(0, I_d)$  and construct  $\tilde{g}_\mu(x_t) = \frac{1}{b} \sum_{i=1}^b \frac{f(x + \tilde{H}_t^{-1/2} u_i) - f(x)}{\mu} \tilde{H}_t^{-1/2} u_i$ ;
  - 7:   Compute  $y_{t+1} = x_t - \eta \tilde{g}_\mu(x_t)$  and set  $N_b = b$ .
  - 8:   **while**  $f(y_{t+1}) > f(x_t)$  and  $N_b < \beta$  **do**
  - 9:     Generate another  $\delta_b$  samples with  $u_i \sim N(0, I_d)$  and set  $N_b = N_b + \delta_b$ ;
  - 10:    Construct  $\tilde{g}_\mu(x_t) = \frac{1}{N_b} \sum_{i=1}^{N_b} \frac{f(x + \tilde{H}_t^{-1/2} u_i) - f(x)}{\mu} \tilde{H}_t^{-1/2} u_i$ ;
  - 11:    Compute  $y_{t+1} = x_t - \eta \tilde{g}_\mu(x_t)$ .
  - 12:   **end while**
  - 13:   Update  $x_{t+1} = x_t - \eta \tilde{g}_\mu(x_t)$ .
  - 14: **end for**
- 

### 5.1.1 Descent Checking

To improve the success rate and the query efficiency, we introduce an important technique called **Descent-Checking** which has been discussed in Remark 1 but with a slight different implementation. **Descent-Checking** has the following algorithmic procedure. After obtaining the  $x_{t+1}$ , we will query to the value  $f(x_{t+1})$  and check if  $f(x_{t+1}) \leq f(x_t)$ . If it holds, we will go to the next iteration. Otherwise, we will discard current  $x_{t+1}$  and take extra  $\delta_b$  samples combining with existing samples to estimate a new gradient until a new  $x_{t+1}$  satisfies  $f(x_{t+1}) \leq f(x_t)$  or the total sample size exceeds a threshold. If the total sample size exceeds the threshold, we will accept this ‘bad’  $x_{t+1}$  and go to the next iteration. Because we will often set  $b$  be of several tens, **Descent-Checking** strategy will not bring many extra queries. As a result of **Descent-Checking**, we can filter some bad search direction effectively which will lead to a higher attack success rate. We depict the detailed algorithmic procedure of ZO-HessAware with **Descent-Checking** in Algorithm 3. Accordingly, we name ZOHA-Gauss and ZOHA-Diag with **Descent-Checking** strategy as ZOHA-Gauss-DC and ZOHA-Diag-DC, respectively.

## 5.2 Evaluation on MNIST

We evaluate the effectiveness of our attacks against an convolution neural network (CNN) on the MNIST dataset. The network for MNIST is composed of two  $5 \times 5$  convolutional layers with output 16 and 64 channels following two fully connected layers with 128 and 10 units. We use  $2 \times 2$  max-pooling after each convolutional layer and use ReLU after every layer expect the layer. The network is trained for 100 epochs with learning rate starting at 0.1 and decay 0.5 every 20 epochs. The accuracy of the model is 98.95%.

We test the attack algorithms on 10000 images from the test set. The limit of  $\ell_\infty$  perturbation is  $\varepsilon = 0.2$ . We run all the attack until getting the an adversarial examples unless the number of



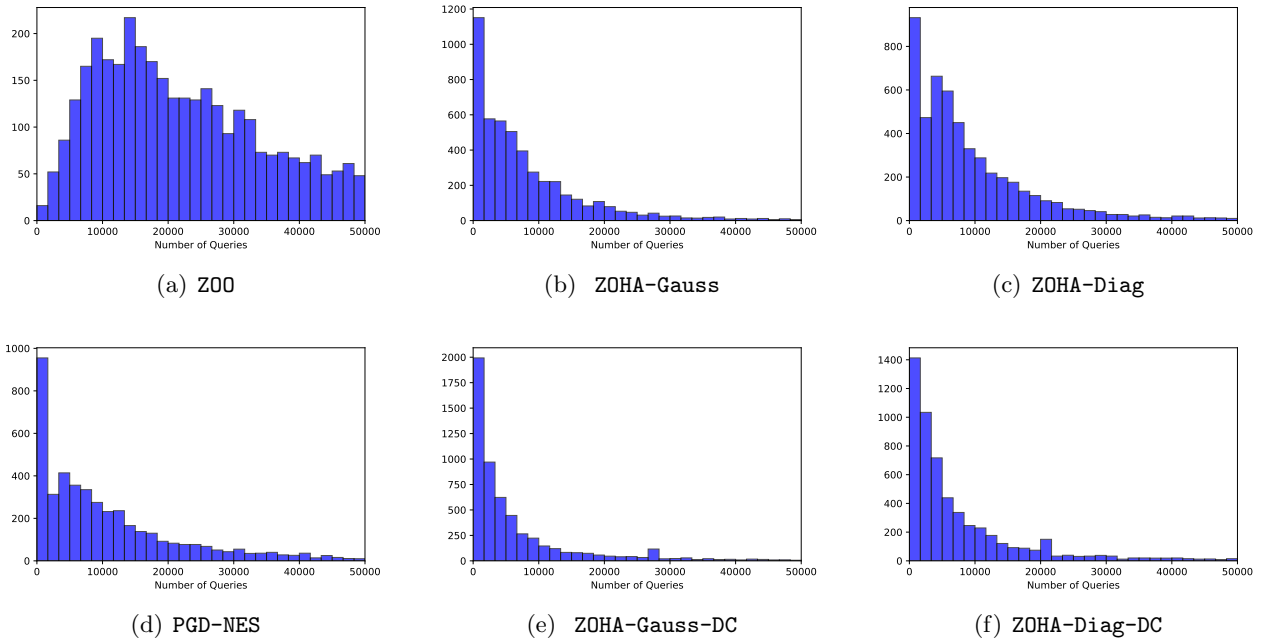


Figure 1: The distribution of the number of queries on *targeted* black-box attacks on CNN model and MNIST

queries is more than 50,000. The parameter settings of algorithms is listed in Table 3 in Appendix. Furthermore, in ZOHA-Gauss and ZOHA-Gauss-DC, we update approximate Hessian once every  $p = 20$  iterations and  $\mu = 0.5$  in Eqn. (4.1). To make a fair comparison, we do not add ‘momentum’ which is an effective technique to reduce queries to all algorithms including ZOHA-type algorithms, PGD-NES, and ZOO.

We report the experiment results in Table 1 and Figure 1 and 2. The visualization of adversarial attack is present in Appendix F. We can observe that ZO-HessAware with different implementations obtain much better success rates than two state-of-the-art algorithms. This validates the effectiveness of second-order information of model function in zeroth-order optimization. Especially, our ZOHA-DC type algorithms obtain the best success rates both target and un-target adversarial attacks which are much higher than ZOO and PGD-NES while taking less queries to function values. Furthermore, on the un-target attack, ZOHA-DC type algorithms only take less than half of queries of PGD-NES. This greatly shows the query efficiency of our Hessian-aware zeroth-order algorithm.

The comparison of the distribution of the query number in Figure 1 and 2 shows that Descent Checking technique can reduce the query number effectively. For example, comparing ZOHA-Gauss with ZOHA-Gauss-DC in Figure 2, we can observe that the percentage of the query number between 0 and 2000 of ZOHA-Gauss-DC is much higher than the one of ZOHA-Gauss.

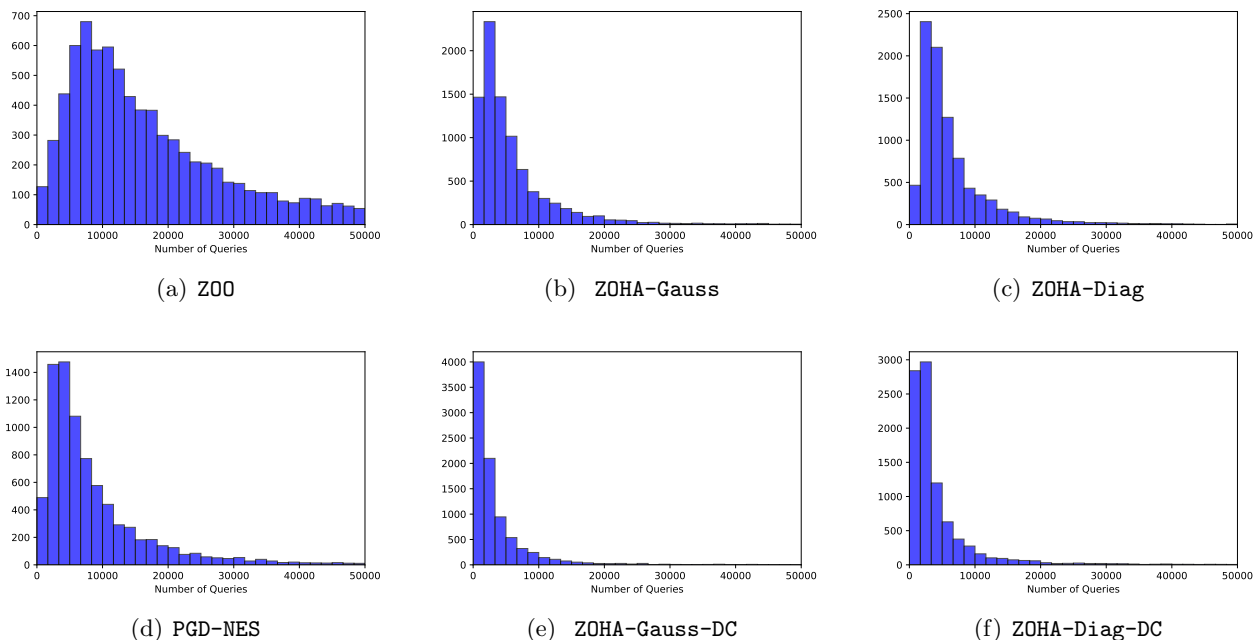


Figure 2: The distribution of the number of queries on *un-targeted* black-box attacks on CNN model and MNIST

### 5.3 Evaluation on ImageNet

In this experiment, we use a pre-trained ResNet50 that has 78.15% top-1 accuracy and 92.87% top-5 accuracy for evaluation. The limit of  $\ell_\infty$  perturbation is  $\varepsilon = 0.05$ . We will choose 1,000 images randomly from ImageNet test-set for evaluation and run the attack method until getting an adversarial example or the number of queries being more than 1,000,000. Furthermore, if the attack is targeted, the target label will be randomly chosen from 1,000 classes. The parameter settings of algorithms is listed in Table 4 in Appendix. Furthermore, in ZOHA-Gauss and ZOHA-Gauss-DC, we update approximate Hessian once every  $p = 20$  iterations and  $\mu = 0.5$  in Eqn. (4.1). To make a fair comparison, we do not add ‘momentum’ which is an effective technique to reduce queries to all algorithms including ZOHA-type algorithms, PGD-NES, and ZOO.

In the experiment on ImageNet, instead of Eqn. (3.2), we use the following method to estimate the gradient

$$g_\mu(x) = \frac{1}{b} \sum_{i=1}^b \frac{f(x + \mu \tilde{H}^{-1/2} u_i) - f(x - \mu \tilde{H}^{-1/2} u_i)}{2\mu} \tilde{H}^{1/2} u_i.$$

We can see that such  $g_\mu$  have the same expectation with the one defined in Eqn. (3.2). However, it has a better performance in this experiment. Accordingly, the natural gradient  $\tilde{g}_\mu(x)$  is modified

Table 1: Comparison of  $\ell_\infty$  norm based black-box attacks on CNN model and MNIST with  $\varepsilon = 0.2$

	Algorithm	success rate %	median queries	average queries
targeted	ZOO (Chen et al., 2017)	42.13	15,200	17,091
	PGD-NES (Ilyas et al., 2018)	44.19	7,300	10,496
	ZOHA-Gauss	50.03	3,712	6,649
	ZOHA-Gauss-DC	<b>56.14</b>	<b>2,941</b>	<b>6,246</b>
	ZOHA-Diag	52.13	6,400	9,128
	ZOHA-Diag-DC	55.56	3,936	7,239
un-targeted	ZOO (Chen et al., 2017)	77.18	13,300	16,390
	PGD-NES (Ilyas et al., 2018)	81.55	5,800	8,567
	ZOHA-Gauss	85.06	3,612	5,000
	ZOHA-Gauss-DC	88.80	<b>2,152</b>	<b>3,629</b>
	ZOHA-Diag	90.37	4,500	6,439
	ZOHA-Diag-DC	<b>91.90</b>	2,460	4,352

similarly as

$$\tilde{g}_\mu(x) = \frac{1}{b} \sum_{i=1}^b \frac{f(x + \mu\tilde{u}_i) - f(x - \mu\tilde{u}_i)}{2\mu} \tilde{u}_i, \text{ with } \tilde{u}_i \sim N(0, \tilde{H}^{-1}).$$

We report the results in Table 2 and Figure 3, 4. The visualization of adversarial attack is present in Figure 6 and 7 of Appendix F. We can observe that our algorithms take much less queries than ZOO and PGD-NES. For the un-target attack, the median queries of ZOHA-Diag-DC is only about 5% of ZOO and about 38% of PGD-NES with the same success rate. For the target attack, compared with the un-target attack problem, all these algorithms take much more queries. But our algorithms still show great query efficiency. Especially, both ZOHA-Diag and ZOHA-Diag-DC achieve 100% attack success rate which is higher than PGD-NES but only with about 50% queries of PGD-NES. Though ZOO also obtain a 100% success rate, it takes several times of queries as ZOHA-Diag and ZOHA-Diag-DC.

## 5.4 Discussion

From above two experiments, we can find some important insights. First, the comparison between attack success rates of two deep learning models indicates that a deeper or more complicate neural network potentially involves more vulnerability to the adversarial attack. On the ResNet50, all algorithms achieve success rates over 99%. In contrast, the attack success rate on the simple convolution network with several layers is much lower.

Second, the great gap of success rates between our Hessian-aware zeroth-order methods and two state-of-the-art algorithms on the MNIST may reveal such a potential that the Hessian information will bring great advantages on the hard adversarial attack problem.

Third, we can observe that our algorithms with `Descent-Checking` have better performance than the ones without `Descent-Checking`. The experiment results on the MNIST show that

Table 2: Comparison of  $\ell_\infty$  norm based black-box attacks on ResNet50 model and ImageNet with  $\varepsilon = 0.05$

	Algorithm	success rate %	median queries	average queries
targeted	ZOO (Chen et al., 2017)	<b>100</b>	39,100	45,822
	PGD-NES (Ilyas et al., 2018)	99.37	11,270	17,435
	ZOHA-Gauss	99.62	8,748	12,257
	ZOHA-Gauss-DC	100	8,588	11,770
	ZOHA-Diag	<b>100</b>	7,400	9,123
	ZOHA-Diag-DC	<b>100</b>	<b>6,273</b>	<b>8,574</b>
un-targeted	ZOO (Chen et al., 2017)	100	12,700	14,199
	PGD-NES (Ilyas et al., 2018)	100	1,500	2,283
	ZOHA-Gauss	100	1,212	2,259
	ZOHA-Gauss-DC	100	1,124	1,959
	ZOHA-Diag	100	800	1,149
	ZOHA-Diag-DC	100	<b>561</b>	<b>945</b>

**Descent-Checking** strategy can promote attack success rate effectively both for targeted and un-targeted attack. At the same time, **Descent-Checking** is an effective way to reduce query complexity. This can be easily observed from the distribution of the number of queries in Figure 1-4.

## 6 Conclusion

In this paper, we propose a novel zeroth-order algorithmic framework called **ZO-HessAware** which exploits the second-order Hessian information of the model function. **ZO-HessAware** achieves a faster convergence rate and lower query complexity than vanilla zeroth-order algorithms that does *not* use the second-order information. Simultaneously, we propose several novel query-efficient approaches to capture the dominant information of the Hessian. Experiments on the black-box adversarial attack show that our **ZO-HessAware** algorithms improve the attack success rate and reduce the query complexity effectively. This validates the effectiveness of the Hessian information in zeroth-order optimization and our theoretical analysis empirically. We also propose a technique called **Descent-Checking** which can empirically further promote attack success rate and reduce query complexity.

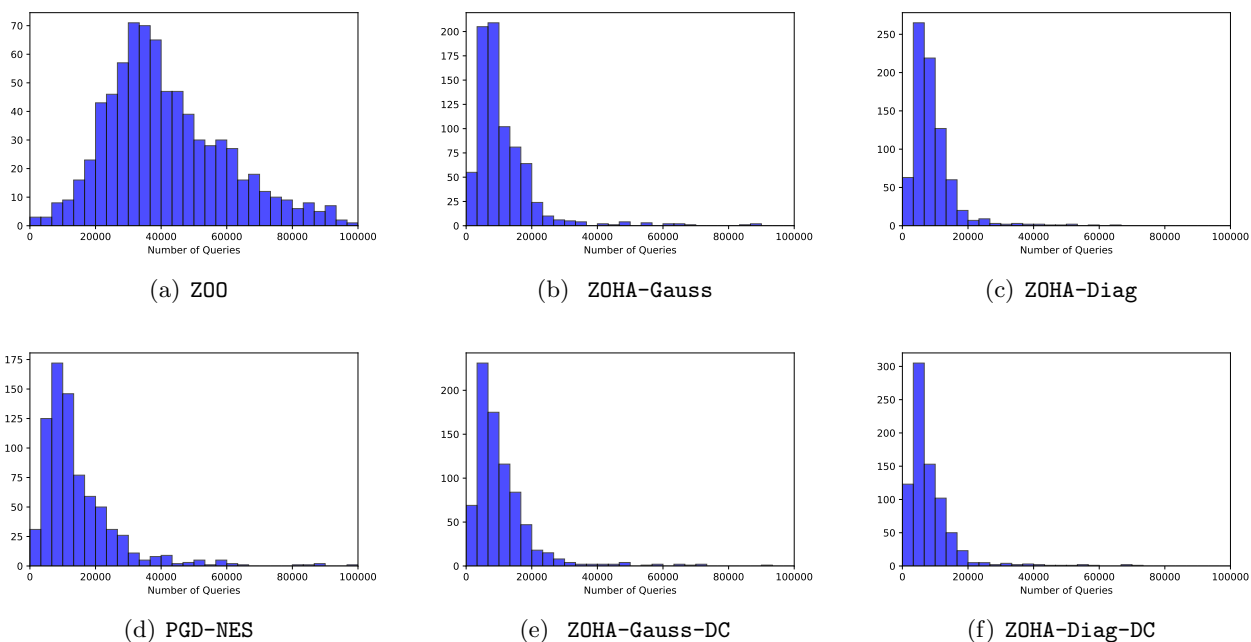


Figure 3: The distribution of the number of queries on *targeted* black-box attacks on ResNet50 model and ImageNet

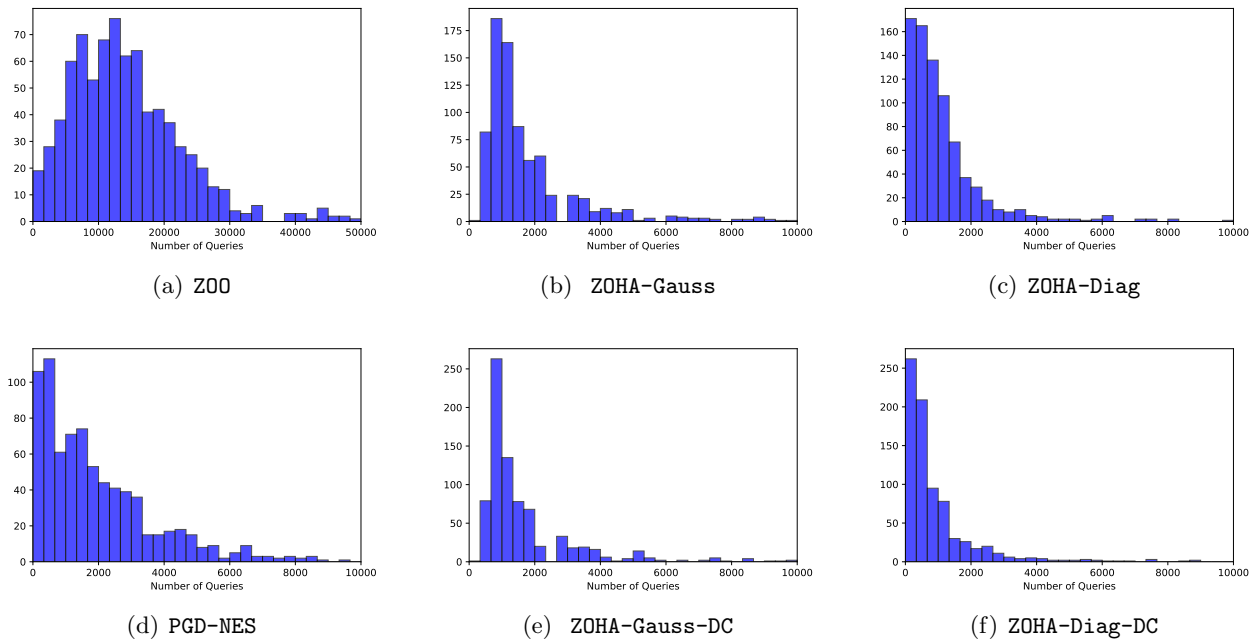


Figure 4: The distribution of the number of queries on *un-targeted* black-box attacks on ResNet50 model and ImageNet

## References

- Bach, F. & Perchet, V. (2016). Highly-smooth zero-th order online optimization. In *Conference on Learning Theory* (pp. 257–283).
- Bakker, C., Henry, M. J., & Hodas, N. O. (2018). Understanding and exploiting the low-rank structure of deep networks.
- Balcan, M.-F., Du, S. S., Wang, Y., & Yu, A. W. (2016). An improved gap-dependency analysis of the noisy power method. In *Conference on Learning Theory* (pp. 284–309).
- Bergstra, J. S., Bardenet, R., Bengio, Y., & Kégl, B. (2011). Algorithms for hyper-parameter optimization. In *Advances in neural information processing systems* (pp. 2546–2554).
- Carlini, N. & Wagner, D. (2017). Towards evaluating the robustness of neural networks. In *2017 IEEE Symposium on Security and Privacy (SP)* (pp. 39–57).: IEEE.
- Chen, P.-Y., Zhang, H., Sharma, Y., Yi, J., & Hsieh, C.-J. (2017). Zoo: Zeroth order optimization based black-box attacks to deep neural networks without training substitute models. In *Proceedings of the 10th ACM Workshop on Artificial Intelligence and Security* (pp. 15–26).: ACM.
- Duchi, J., Hazan, E., & Singer, Y. (2011). Adaptive subgradient methods for online learning and stochastic optimization. *Journal of Machine Learning Research*, 12(Jul), 2121–2159.
- Duchi, J. C., Jordan, M. I., Wainwright, M. J., & Wibisono, A. (2015). Optimal rates for zero-order convex optimization: The power of two function evaluations. *IEEE Transactions on Information Theory*, 61(5), 2788–2806.
- Fang, C., Li, C. J., Lin, Z., & Zhang, T. (2018). Spider: Near-optimal non-convex optimization via stochastic path-integrated differential estimator. In *Advances in Neural Information Processing Systems* (pp. 686–696).
- Ghadimi, S. & Lan, G. (2013). Stochastic first-and zeroth-order methods for nonconvex stochastic programming. *SIAM Journal on Optimization*, 23(4), 2341–2368.
- Hansen, N. & Ostermeier, A. (2001). Completely derandomized self-adaptation in evolution strategies. *Evolutionary computation*, 9(2), 159–195.
- Hu, W. & Tan, Y. (2017). Generating adversarial malware examples for black-box attacks based on gan. *arXiv preprint arXiv:1702.05983*.
- Ilyas, A., Engstrom, L., Athalye, A., & Lin, J. (2018). Black-box adversarial attacks with limited queries and information. In J. Dy & A. Krause (Eds.), *Proceedings of the 35th International Conference on Machine Learning*, volume 80 of *Proceedings of Machine Learning Research* (pp. 2137–2146). Stockholmsmässan, Stockholm Sweden: PMLR.
- Kingma, D. P. & Ba, J. (2015). Adam: A method for stochastic optimization. In *International Conference on Learning Representations (ICLR)*.

- Liu, S., Kailkhura, B., Chen, P.-Y., Ting, P., Chang, S., & Amini, L. (2018). Zeroth-order stochastic variance reduction for nonconvex optimization. In S. Bengio, H. Wallach, H. Larochelle, K. Grauman, N. Cesa-Bianchi, & R. Garnett (Eds.), *Advances in Neural Information Processing Systems 31* (pp. 3731–3741). Curran Associates, Inc.
- Magnus, J. R. (1978). The moments of products of quadratic forms in normal variables. *Statistica Neerlandica*, 32(4), 201–210.
- Matyas, J. (1965). Random optimization. *Automation and Remote control*, 26(2), 246–253.
- Nesterov, Y. & Spokoiny, V. (2017). Random gradient-free minimization of convex functions. *Foundations of Computational Mathematics*, 17(2), 527–566.
- Papernot, N., McDaniel, P., Goodfellow, I., Jha, S., Celik, Z. B., & Swami, A. (2017). Practical black-box attacks against machine learning. In *Proceedings of the 2017 ACM on Asia Conference on Computer and Communications Security* (pp. 506–519).: ACM.
- Sainath, T. N., Kingsbury, B., Sindhvani, V., Arisoy, E., & Ramabhadran, B. (2013). Low-rank matrix factorization for deep neural network training with high-dimensional output targets. In *Acoustics, Speech and Signal Processing (ICASSP), 2013 IEEE International Conference on* (pp. 6655–6659).: IEEE.
- Salimans, T., Ho, J., Chen, X., Sidor, S., & Sutskever, I. (2017). Evolution strategies as a scalable alternative to reinforcement learning. *arXiv preprint arXiv:1703.03864*.
- Shamir, O. (2017). An optimal algorithm for bandit and zero-order convex optimization with two-point feedback. *Journal of Machine Learning Research*, 18(52), 1–11.
- Snoek, J., Larochelle, H., & Adams, R. P. (2012). Practical bayesian optimization of machine learning algorithms. In *Advances in neural information processing systems* (pp. 2951–2959).
- Tieleman, T. & Hinton, G. (2012). Lecture 6.5-rmsprop: Divide the gradient by a running average of its recent magnitude. *COURSERA: Neural networks for machine learning*, 4(2), 26–31.
- Wierstra, D., Schaul, T., Glasmachers, T., Sun, Y., Peters, J., & Schmidhuber, J. (2014). Natural evolution strategies. *The Journal of Machine Learning Research*, 15(1), 949–980.
- Yuan, M., Ekici, A., Lu, Z., & Monteiro, R. (2007). Dimension reduction and coefficient estimation in multivariate linear regression. *Journal of the Royal Statistical Society: Series B (Statistical Methodology)*, 69(3), 329–346.
- Zeiler, M. D. (2012). Adadelta: an adaptive learning rate method. *arXiv preprint arXiv:1212.5701*.

## A Proof of Section 3.1

In this section, we will prove three properties of the estimated gradient defined in Eqn. (3.2). Before that, we first list some important lemmas related to the Gaussian distribution that will be used in our proof.

### A.1 Important Lemmas

**Lemma 6** ((Nesterov & Spokoiny, 2017)). *If  $f(x)$  is  $L$ -smooth, then we have*

$$\|\nabla f_\mu(y) - \nabla f_\mu(x)\| \leq L \|x - y\|.$$

**Lemma 7** ((Nesterov & Spokoiny, 2017)). *If  $f(x)$  is  $L$ -smooth, then*

$$\|\nabla f_\mu(x) - \nabla f(x)\| \leq \frac{\mu}{2} L(d+3)^{3/2}.$$

*If the Hessian is  $\gamma$ -Lipschitz continuous, then we can guarantee that*

$$\|\nabla^2 f_\mu(x) - \nabla^2 f(x)\| \leq \frac{\mu^2}{6} \gamma(d+4)^2.$$

**Lemma 8** ((Nesterov & Spokoiny, 2017)). *Let  $p \geq 2$ ,  $u$  be from  $N(0, I_d)$ , then we have the following bound*

$$d^{p/2} \leq \mathbb{E}_u [\|u\|^p] \leq (p+d)^{p/2}.$$

Then we give the results of moments of products quadratic forms in normal distribution.

**Lemma 9** ((Magnus, 1978)). *Let  $A$  and  $B$  be two symmetric matrices, and  $u$  has the Gaussian distribution, that is,  $u \sim N(0, I_d)$ . Define  $z = u^\top A u \cdot u^\top B u$ . The expectation of  $z$  and  $z^2$  are:*

$$\begin{aligned} \mathbb{E}_u(z) &= (\text{tr } A)(\text{tr } B) + 2(\text{tr } AB) \\ \mathbb{E}_u(z^2) &= (\text{tr } A)^2(\text{tr } B)^2 + 16 [(\text{tr } A)(\text{tr } AB^2) + (\text{tr } B)(\text{tr } A^2B)] \\ &\quad + 2 [(\text{tr } A)^2(\text{tr } B)^2 + 4(\text{tr } A)(\text{tr } B)(\text{tr } AB) + (\text{tr } B)^2(\text{tr } A^2)] \\ &\quad + 4 [(\text{tr } A^2)(\text{tr } B^2) + 2(\text{tr } AB)^2] + 16 [(\text{tr } AB)^2 + 2(\text{tr } A^2B^2)]. \end{aligned}$$

### A.2 Proof of Lemma 1

*Proof of Lemma 1.* First, the gradient of  $f_\mu(x)$  can be represented as (Nesterov & Spokoiny, 2017):

$$\begin{aligned} \nabla f_\mu(x) &= \frac{1}{M} \int_{\mathbb{R}^d} \frac{f(x + \mu u) - f(x)}{\mu} u \exp\left(-\frac{\|u\|^2}{2}\right) du \\ &= \mathbb{E}_u \left[ \frac{f(x + \mu u) - f(x)}{\mu} u \right] \end{aligned} \tag{A.1}$$



Let us denote

$$h(y) \triangleq f(x + Ky).$$

Then we have

$$f(x) = h(0).$$

By Eqn. (A.1), we have

$$\mathbb{E}_u \frac{f(x + \mu Ku) - f(x)}{\mu} = \mathbb{E}_u \frac{h(0 + \mu u) - h(0)}{\mu} = \nabla h_\mu(0).$$

And we also have

$$\nabla h(0) = K \cdot \nabla f(x)$$

By Lemma 7, we can obtain that

$$\|\nabla h_\mu(0) - \nabla h(0)\| \leq \frac{\mu}{2} L(h_\mu) (d+3)^{3/2}. \quad (\text{A.2})$$

where  $L(h_\mu)$  is the smoothness parameter of  $h_\mu(y)$ . By Lemma 6, we know that  $L(h_\mu)$  is no larger than the one of  $h(y)$ . And  $L(h)$  has the following upper bound:

$$L(h) \leq L(f) \|K\|^2 = L \|K\|^2.$$

Therefore, we have

$$\begin{aligned} \|\mathbb{E}_u [g_\mu(x)] - \nabla f(x)\|_{K^2}^2 &= \|K^{-1}(\nabla h_\mu(0) - \nabla h(0))\|_{K^2}^2 \\ &= \|\nabla h_\mu(0) - \nabla h(0)\|^2 \\ &\leq \frac{\mu^2}{4} L^2 \|K\|^4 (d+3)^3. \end{aligned}$$

□

### A.3 Proof of Lemma 2

*Proof of Lemma 2.* By the definition of  $g_\mu(x)$ , we have

$$\begin{aligned}
\mathbb{E}_u \|g_\mu(x)\|_{K^2}^2 &= \frac{1}{\mu^2 b^2} \mathbb{E} \left\| \left( \sum_{i=1}^b [f(x + \mu K u_i) - f(x)] K^{-1} u_i \right) \right\|_{K^2}^2 \\
&= \frac{1}{\mu^2 b^2} \mathbb{E}_{u_i, u_j} \sum_{i,j} (f(x + \mu K u_i) - f(x)) (f(x + \mu K u_j) - f(x)) u_i u_j \\
&= \frac{1}{\mu^2 b} \mathbb{E}_u \left( [f(x + \mu K u) - f(x)]^2 \|K^{-1} u\|_{K^2}^2 \right) \\
&\quad + \frac{1}{\mu^2 b^2} \sum_{i \neq j} (\mathbb{E}_{u_i} (f(x + \mu K u_i) - f(x)) u_i) (\mathbb{E}_{u_j} (f(x + \mu K u_j) - f(x)) u_j) \\
&= \frac{1}{\mu^2 b} \mathbb{E}_u \left( [f(x + \mu K u) - f(x)]^2 \|K^{-1} u\|_{K^2}^2 \right) + \frac{b^2 - b}{b^2} \|\mathbb{E}[g_\mu(x)]\|_{K^2}^2 \\
&\leq \frac{1}{\mu^2 b} \mathbb{E}_u \left( [f(x + \mu K u) - f(x)]^2 \|K^{-1} u\|_{K^2}^2 \right) + 2 \|\nabla f(x)\|_{K^2}^2 + \frac{\mu^2 L^2 (d+3)^3}{2}
\end{aligned}$$

The first equality is because  $u_i$ 's are independent, and we have

$$\begin{aligned}
[f(x + \mu K u) - f(x)]^2 &= [f(x + \mu K u) - f(x) - \mu \langle \nabla f(x), K u \rangle + \mu \langle \nabla f(x), K u \rangle]^2 \\
&\leq 2 \left[ \frac{\mu^2}{2} L \|K\|^2 \|u\|^2 \right]^2 + 2\mu^2 \langle \nabla f(x), K u \rangle^2
\end{aligned}$$

where the last inequality is from Lemma 1. We can also obtain that

$$\begin{aligned}
\mathbb{E}_u \left[ \langle K \nabla f(x), u \rangle^2 \|K^{-1} u\|_{K^2}^2 \right] &= \mathbb{E}_u \left[ u^\top K \nabla f(x) \nabla f(x)^\top K^\top u \cdot u^\top K^{-1} K^2 K^{-1} u \right] \\
&= (\text{tr } K \nabla f(x) \nabla f(x)^\top K^\top) (\text{tr } I) + 2 \text{tr}(K \nabla f(x) \nabla f(x)^\top K^\top) \\
&= d \|\nabla f(x)\|_{K^2}^2 + 2 \|\nabla f(x)\|_{K^2}^2 \\
&= (d+2) \|\nabla f(x)\|_{K^2}^2,
\end{aligned}$$

where the second equation is because of Lemma 9 with  $A = K \nabla f(x) \nabla f(x)^\top K^\top$  and  $B = K^{-1} K^2 K^{-1} = I$ . Therefore, we have

$$\begin{aligned}
&\mathbb{E}_u \|g_\mu(x)\|_{K^2}^2 \\
&\leq \frac{\mu^2}{2b} L^2 \|K\|^4 \mathbb{E}_u \left[ \|u\|^4 \cdot \|K^{-1} u\|_{K^2}^2 \right] + \frac{1}{b} \cdot \mathbb{E}_u \left[ \langle K \nabla f(x), u \rangle^2 \|K^{-1} u\|_{K^2}^2 \right] + 2 \|\nabla f(x)\|_{K^2}^2 + \frac{\mu^2 L^2 (d+3)^3}{2} \\
&\leq \frac{\mu^2}{2b} L^2 \|K\|^4 \mathbb{E}_u \left[ \|u\|^6 \right] + \left( \frac{2(d+2)}{b} + 2 \right) \cdot \|\nabla f(x)\|_{K^2}^2 + \frac{\mu^2 L^2 (d+3)^3}{2} \\
&\leq \frac{\mu^2}{2b} L^2 \|K\|^4 (d+6)^3 + \left( \frac{2(d+2)}{b} + 2 \right) \cdot \|\nabla f(x)\|_{K^2}^2 + \frac{\mu^2 L^2 (d+3)^3}{2}, \tag{A.3}
\end{aligned}$$

where the last inequality is due to Lemma 8.  $\square$

## A.4 Proof of Lemma 3

*Proof of Lemma 3.* First, we have

$$\begin{aligned}\mathbb{E}_u \|K^2 g_\mu(x)\|_{K^{-2}}^3 &\leq \frac{1}{\mu^3 b^3} \cdot b^2 \sum_{i=1}^b \mathbb{E}_{u_i} \left( [f(x + \mu K u_i) - f(x)]^3 \cdot \|K u_i\|_{K^{-2}}^3 \right) \\ &= \frac{1}{\mu^3} \mathbb{E}_u \left( [f(x + \mu K u) - f(x)]^3 \cdot \|u\|^3 \right).\end{aligned}$$

Furthermore, we can obtain that

$$\begin{aligned}[f(x + \mu K u) - f(x)]^3 &= [f(x + \mu K u) - f(x) - \mu \langle \nabla f(x), K u \rangle + \mu \langle \nabla f(x), K u \rangle]^3 \\ &\leq 4 \left[ \frac{\mu^2}{2} L \|K\|^2 \|u\|^2 \right]^3 + 4\mu^3 \langle K \nabla f(x), u \rangle^3,\end{aligned}$$

and we also have

$$\begin{aligned}&\mathbb{E}_u \left[ \|u\|^3 \cdot \langle K \nabla f(x), u \rangle^3 \right] \\ &= \mathbb{E}_u \left[ \left( (u^\top u)^2 \cdot (u^\top K \nabla f(x) \nabla^\top f(x) K u)^2 \right)^{3/4} \right] \\ &\leq \left( \mathbb{E}_u \left[ (u^\top u)^2 \cdot (u^\top K \nabla f(x) \nabla^\top f(x) K u)^2 \right] \right)^{3/4},\end{aligned}$$

where the last inequality is because Jensen's inequality.

Let us denote  $A = K \nabla f(x) \nabla^\top f(x) K$ . It is easy to check that  $A$  is a rank one positive semi-definite matrix, and its trace satisfies that  $\text{tr}(A) = \|\nabla f(x)\|_{K^2}^2$ . By Lemma 9 with  $A = K \nabla f(x) \nabla^\top f(x) K$  and  $B = I$ , we have

$$\begin{aligned}&\mathbb{E}_u \left[ (u^\top u)^2 \cdot (u^\top K \nabla f(x) \nabla^\top f(x) K u)^2 \right] \\ &= (\text{tr } I_d)^2 (\text{tr } A)^2 + 16 [(\text{tr } I_d)(\text{tr } I_d A^2) + (\text{tr } A)(\text{tr } I_d^2 A)] \\ &\quad + 4 [(\text{tr } I_d^2)(\text{tr } A^2) + 2(\text{tr } I_d A)^2] + 2 [(\text{tr } I_d)^2 (\text{tr } A^2) + 4(\text{tr } I_d)(\text{tr } A)(\text{tr } I_d A) \\ &\quad + (\text{tr } A)^2 (\text{tr } I_d^2)] + 16 [\text{tr}(I_d A)^2 + 2(\text{tr } I_d^2 A^2)] \\ &= d^2 \|\nabla f(x)\|_{K^2}^4 + 16 \left[ d \|\nabla f(x)\|_{K^2}^4 + \|\nabla f(x)\|_{K^2}^4 \right] + 4 \left[ d \|\nabla f(x)\|_{K^2}^4 + 2 \|\nabla f(x)\|_{K^2}^4 \right] \\ &\quad + 2 \left[ d^2 \|\nabla f(x)\|_{K^2}^4 + 4d \|\nabla f(x)\|_{K^2}^4 + d \|\nabla f(x)\|_{K^2}^4 \right] + 16 \left[ \|\nabla f(x)\|_{K^2}^4 + 2 \|\nabla f(x)\|_{K^2}^4 \right] \\ &= (3d^2 + 30d + 72) \cdot \|\nabla f(x)\|_{K^2}^4.\end{aligned}$$

Thus, we can obtain that

$$\begin{aligned}
\mathbb{E}_u \left[ \|u\|^3 \cdot \langle K \nabla f(x), u \rangle^3 \right] &\leq \left( \mathbb{E}_u \left[ (u^\top u)^2 \cdot (u^\top K \nabla f(x) \nabla^\top f(x) K u)^2 \right] \right)^{3/4} \\
&\leq \left( (3d^2 + 30d + 72) \cdot \|\nabla f(x)\|_{K^2}^4 \right)^{3/4} \\
&\leq \left( 3(d+5)^2 \cdot \|\nabla f(x)\|_{K^2}^4 \right)^{3/4} \\
&\leq 3(d+5)^{3/2} \|\nabla f(x)\|_{K^2}^3.
\end{aligned}$$

Therefore, we have

$$\begin{aligned}
\mathbb{E}_u \|K^2 g_\mu(x)\|_{K^{-2}}^3 &\leq \frac{1}{\mu^3} \mathbb{E}_u \left( 4 \left[ \frac{\mu^2}{2} L \|K\|^2 \|u\|^2 \right]^3 \|u\|^3 + 4\mu^3 \langle K \nabla f(x), u \rangle^3 \|u\|^3 \right) \\
&\leq \frac{\mu^3 L^3 \|K\|^6}{2} \mathbb{E}_u \left[ \|u\|^9 \right] + 12(d+5)^{3/2} \|\nabla f(x)\|_{K^2}^3 \\
&\leq 2\mu^3 L^3 \|K\|^6 \cdot (d+9)^{9/2} + 12(d+5)^{3/2} \|\nabla f(x)\|_{K^2}^3.
\end{aligned}$$

where the last inequality follows from Lemma 8.  $\square$

## B Proof of Convergence Rate of Algorithm 1

In this section, we will prove the convergence rate of Algorithm 1. Before that, we first give an important lemma which depicts some properties related to the strong convexity.

**Lemma 10.** *Let  $f$  be continuously differentiable and strongly convex with parameter  $\tau$ . And  $x^*$  is the minimizer of  $f$ . Then for any  $x \in \mathbb{R}^d$ , we have*

$$\|\nabla f(x)\|^2 \geq 2\tau(f(x) - f(x^*)),$$

and

$$\|x - x^*\|^2 \leq \frac{2}{\tau}(f(x) - f(x^*)).$$

*Proof.* First, by the strong convexity of  $f$ ,

$$\begin{aligned}
f(x^*) &\geq f(x) + \langle \nabla f(x), x^* - x \rangle + \frac{\tau}{2} \|x^* - x\|^2 \\
&\geq f(x) + \min_v \left( \langle \nabla f(x), v \rangle + \frac{\tau}{2} \|v\|^2 \right) \\
&= f(x) - \frac{1}{2\tau} \|\nabla f(x)\|^2.
\end{aligned}$$

The last equality holds by plugging in the minimizer  $v = -\nabla f(x)/\tau$ .

Also by the strong convexity of  $f$ , we have

$$\begin{aligned} f(x) &\geq f(x^*) + \langle \nabla f(x^*), x - x^* \rangle + \frac{\tau}{2} \|x^* - x\|^2 \\ &= f(x^*) + \frac{\tau}{2} \|x^* - x\|^2. \end{aligned}$$

□

## B.1 Proof of Theorem 1

Now, we give the proof of the local convergence properties depicted in Theorem 1.

*Proof of Theorem 1.* Let  $H$  denote the Hessian  $\nabla^2 f(x_t)$ . Taking a random step from  $x_t$ , we have

$$\begin{aligned} &\mathbb{E}_u [f(x_{t+1})] \\ &= \mathbb{E}_u \left[ f(x_t - \eta \tilde{H}^{-1} g_\mu(x_t)) \right] \\ &\stackrel{(2.5)}{\leq} f(x_t) - \eta \left\langle \nabla f(x_t), \tilde{H}^{-1} \mathbb{E}_u [g_\mu(x_t)] \right\rangle + \frac{\eta^2}{2} \mathbb{E}_u \left\| \tilde{H}^{-1} g_\mu(x_t) \right\|_H^2 + \frac{\eta^3 \gamma}{6} \mathbb{E}_u \left\| \tilde{H}^{-1} g_\mu(x_t) \right\|^3 \\ &\stackrel{(3.1)}{\leq} f(x_t) - \eta \left\| \nabla f(x_t) \right\|_{\tilde{H}^{-1}}^2 - \eta \left\langle \nabla f(x_t), \tilde{H}^{-1} (\mathbb{E}_u [g_\mu(x_t)] - \nabla f(x_t)) \right\rangle \\ &\quad + \eta^2 \mathbb{E}_u \left\| \tilde{H}^{-1} g_\mu(x_t) \right\|_{\tilde{H}}^2 + \frac{\eta^3 \gamma}{6} \mathbb{E}_u \left\| \tilde{H}^{-1} g_\mu(x_t) \right\|^3 \\ &\leq f(x_t) - \eta \left\| \nabla f(x_t) \right\|_{\tilde{H}^{-1}}^2 + \frac{\eta}{2} \left( \left\| \nabla f(x_t) \right\|_{\tilde{H}^{-1}}^2 + \left\| \mathbb{E}_u [g_\mu(x_t)] - \nabla f(x_t) \right\|_{\tilde{H}^{-1}}^2 \right) \\ &\quad + \eta^2 \mathbb{E}_u \left\| \tilde{H}^{-1} g_\mu(x_t) \right\|_{\tilde{H}}^2 + \frac{\eta^3 \gamma}{6} \mathbb{E}_u \left\| \tilde{H}^{-1} g_\mu(x_t) \right\|^3 \\ &= f(x_t) - \frac{\eta}{2} \left\| \nabla f(x_t) \right\|_{\tilde{H}^{-1}}^2 + \underbrace{\frac{\eta}{2} \left\| \mathbb{E}_u [g_\mu(x_t)] - \nabla f(x_t) \right\|_{\tilde{H}^{-1}}^2}_{T_1} + \underbrace{\eta^2 \mathbb{E}_u \left\| \tilde{H}^{-1} g_\mu(x_t) \right\|_{\tilde{H}}^2}_{T_2} \\ &\quad + \underbrace{\frac{\eta^3 \gamma}{6} \mathbb{E}_u \left\| \tilde{H}^{-1} g_\mu(x_t) \right\|^3}_{T_3}, \end{aligned} \tag{B.1}$$

where inequality (B.1) follows from Cauchy's Inequality.

Now we begin to bound terms  $T_1$ ,  $T_2$ , and  $T_3$ . First, by Lemma 1 with  $K = \tilde{H}^{-1/2}$ , we have

$$\left\| \mathbb{E}_u [g_\mu(x_t)] - \nabla f(x_t) \right\|_{\tilde{H}^{-1}}^2 = \left\| \mathbb{E}_u [g_\mu(x_t)] - \nabla f(x_t) \right\|_{K^2}^2 \leq \frac{\mu^2 L^2}{4} \left\| \tilde{H}^{-1} \right\|^2 (d+3)^3,$$

that is,

$$T_1 \leq \frac{\eta \mu^2 L^2}{8} \left\| \tilde{H}^{-1} \right\|^2 (d+3)^3.$$

By Lemma 2 with  $K = \tilde{H}^{-1/2}$ , we have

$$\begin{aligned} \mathbb{E}_u \left\| \tilde{H}^{-1} g_\mu(x_t) \right\|_{\tilde{H}}^2 &= \mathbb{E}_u \|g_\mu(x_t)\|_{\tilde{H}^{-1}}^2 \\ &\leq \frac{\mu^2}{2b} L^2 \left\| \tilde{H}^{-1} \right\|^2 (d+6)^3 + \left( \frac{2(d+2)}{b} + 2 \right) \|\nabla f(x)\|_{\tilde{H}^{-1}}^2 + \frac{\mu^2 L^2 (d+3)^3}{2}. \end{aligned}$$

Using the condition that  $b \leq d+2$ ,  $T_2$  is upper bounded as

$$T_2 \leq \eta^2 \left( \frac{\mu^2 L^2}{2b} \left\| \tilde{H}^{-1} \right\|^2 (d+6)^3 + \frac{4(d+2)}{b} \|\nabla f(x)\|_{\tilde{H}^{-1}}^2 + \frac{\mu^2 L^2 (d+3)^3}{2} \right).$$

Using Lemma 3, we have

$$\begin{aligned} T_3 &= \frac{\eta^3}{6} \cdot \mathbb{E}_u \left\| \tilde{H}^{-1} g_\mu(x_t) \right\|_{\tilde{H}}^3 \\ &\leq \frac{\eta^3}{6} \cdot \left\| \tilde{H}^{-1} \right\|^{3/2} \cdot \mathbb{E}_u \left\| \tilde{H}^{-1} g_\mu(x_t) \right\|_{\tilde{H}}^3 \\ &\leq \frac{\gamma \mu^3 L^3 \eta^3 \left\| \tilde{H}^{-1} \right\|^{9/2}}{12} \cdot (d+9)^{9/2} + 2\gamma \eta^3 (d+5)^{3/2} \left\| \tilde{H}^{-1} \right\|^{3/2} \cdot \|\nabla f(x)\|_{\tilde{H}^{-1}}^3. \end{aligned}$$

Thus, we have

$$\begin{aligned} &T_1 + T_2 + T_3 \\ &\leq \frac{\eta \mu^2 L^2}{8} \left\| \tilde{H}^{-1} \right\|^2 (d+3)^3 + \frac{\mu^2 L^2 \eta^2}{2b} \left\| \tilde{H}^{-1} \right\|^2 (d+6)^3 + \frac{4(d+2)\eta^2}{b} \|\nabla f(x)\|_{\tilde{H}^{-1}}^2 \\ &\quad + \frac{\eta^2 \mu^2 L^2}{2} (d+3)^3 + \frac{\gamma \mu^3 L^3 \eta^3 \left\| \tilde{H}^{-1} \right\|^{9/2}}{12} \cdot (d+9)^{9/2} + 2\gamma \eta^3 (d+5)^{3/2} \left\| \tilde{H}^{-1} \right\|^{3/2} \cdot \|\nabla f(x)\|_{\tilde{H}^{-1}}^3. \end{aligned}$$

By choosing  $\eta = \frac{b}{16(d+2)}$ , we obtain that

$$\begin{aligned}
& \mathbb{E}_u [f(x_{t+1})] \\
& \leq f(x_t) - \frac{\eta}{2} \|\nabla f(x_t)\|_{\tilde{H}^{-1}}^2 + T_1 + T_2 + T_3 \\
& \leq f(x_t) - \frac{b}{64(d+2)} \|\nabla f(x_t)\|_{\tilde{H}^{-1}}^2 + \frac{\mu^2 L^2 b}{64} \left\| \tilde{H}^{-1} \right\|^2 (d+5)^2 + \frac{b\mu^2 L^2 \left\| \tilde{H}^{-1} \right\|}{128} (d+38) \\
& \quad + \frac{b^3 \gamma \mu^3 L^3 \left\| \tilde{H}^{-1} \right\|^{9/2}}{6144} \cdot (d+110)^{3/2} + \frac{b^2 \mu^2 L^2}{256} (d+7) + \frac{b^3 \gamma}{64} d^{-3/2} \left\| \tilde{H}^{-1} \right\|^{3/2} \cdot \|\nabla f(x)\|_{\tilde{H}^{-1}}^3 \\
& = f(x_t) - \frac{b}{32(d+2)} \|\nabla f(x_t)\|_{\tilde{H}^{-1}}^2 + \frac{b^3 \gamma}{64} d^{-3/2} \left\| \tilde{H}^{-1} \right\|^{3/2} \cdot \|\nabla f(x)\|_{\tilde{H}^{-1}}^3 \\
& \quad + b \cdot \left( \frac{\mu^2 L^2}{64} \left\| \tilde{H}^{-1} \right\|^2 (d+5)^2 + \frac{\mu^2 L^2 \left\| \tilde{H}^{-1} \right\|}{128} (d+38) + \frac{\mu^2 L^2 b}{256} (d+7) + \frac{\gamma b^2 \mu^3 L^3 \left\| \tilde{H}^{-1} \right\|^{9/2}}{6144} \cdot (d+110)^{3/2} \right) \\
& = f(x_t) - \frac{b}{32(d+2)} \|\nabla f(x_t)\|_{\tilde{H}^{-1}}^2 + \frac{b^3 \gamma}{64} d^{-3/2} \left\| \tilde{H}^{-1} \right\|^{3/2} \cdot \|\nabla f(x)\|_{\tilde{H}^{-1}}^3 + \Delta_\mu,
\end{aligned}$$

where we denote

$$\Delta_\mu = b \cdot \left( \frac{\mu^2 L^2}{64} \left\| \tilde{H}^{-1} \right\|^2 (d+5)^2 + \frac{\mu^2 L^2 \left\| \tilde{H}^{-1} \right\|}{128} (d+38) + \frac{\mu^2 L^2 b}{256} (d+7) + \frac{\gamma b^2 \mu^3 L^3 \left\| \tilde{H}^{-1} \right\|^{9/2}}{6144} \cdot (d+110)^{3/2} \right).$$

Now, we begin to give the connections between  $\|\nabla f(x_t)\|_{\tilde{H}^{-1}}^2$  and  $f(x_t) - f(x^*)$ . First, by the Taylor's expansion, we have

$$\begin{aligned}
\nabla f(x_t) &= \nabla f(x^*) + \nabla^2 f(x^*)(x_t - x^*) + \int_0^1 (\nabla^2 f(x^* + s(x_t - x^*)) - \nabla^2 f(x^*)) (x_t - x^*) ds \\
&= \nabla^2 f(x^*)(x_t - x^*) + \Delta_1.
\end{aligned}$$

where the last equation is because  $\nabla f(x^*) = 0$  and we denote that

$$\Delta_1 \triangleq \int_0^1 (\nabla^2 f(x^* + s(x_t - x^*)) - \nabla^2 f(x^*)) (x_t - x^*) ds,$$

and  $\|\Delta_1\|$  is upper bounded as

$$\|\Delta_1\| \leq \rho \int_0^1 s \|x_t - x^*\|^2 ds = \frac{\rho}{2} \|x_t - x^*\|^2. \tag{B.2}$$

Let us denote  $H_\star = \nabla^2 f(x^\star)$ . We have

$$\begin{aligned}
& - \|\nabla f(x_t)\|_{\tilde{H}^{-1}}^2 \\
&= - \|H_\star(x_t - x^\star) + \Delta_1\|_{\tilde{H}^{-1}}^2 \\
&= - \|H(x_t - x^\star) + \Delta_1 + (H_\star - H)(x_t - x^\star)\|_{\tilde{H}^{-1}}^2 \\
&\leq - \left( \|H(x_t - x^\star)\|_{\tilde{H}^{-1}}^2 + \|\Delta_1\|_{\tilde{H}^{-1}}^2 + \|(H_\star - H)(x_t - x^\star)\|_{\tilde{H}^{-1}}^2 \right) \\
&\quad + 2 \left( \|H(x_t - x^\star)\|_{\tilde{H}^{-1}} \cdot \|\Delta_1\|_{\tilde{H}^{-1}} + \|\Delta_1\|_{\tilde{H}^{-1}} \cdot \|(H_\star - H)(x_t - x^\star)\|_{\tilde{H}^{-1}} \right. \\
&\quad \left. + \|(H_\star - H)(x_t - x^\star)\|_{\tilde{H}^{-1}} \cdot \|H(x_t - x^\star)\|_{\tilde{H}^{-1}} \right) \\
&\leq -\rho \|x_t - x^\star\|_H^2 + \Delta_2.
\end{aligned}$$

where the last inequality is because of the condition that  $\rho\tilde{H} \preceq H$  and we denote that

$$\begin{aligned}
\Delta_2 = & 2 \|H(x_t - x^\star)\|_{\tilde{H}^{-1}} \cdot \|\Delta_1\|_{\tilde{H}^{-1}} + 2 \|\Delta_1\|_{\tilde{H}^{-1}} \cdot \|(H_\star - H)(x_t - x^\star)\|_{\tilde{H}^{-1}} \\
& + 2 \|(H_\star - H)(x_t - x^\star)\|_{\tilde{H}^{-1}} \cdot \|H(x_t - x^\star)\|_{\tilde{H}^{-1}}.
\end{aligned}$$

Furthermore, we have

$$\begin{aligned}
f(x_t) &\stackrel{(2.5)}{\leq} f(x^\star) + \langle \nabla f(x^\star), x_t - x^\star \rangle + \frac{1}{2} \langle \nabla^2 f(x^\star)(x_t - x^\star), x_t - x^\star \rangle + \frac{\gamma}{6} \|x_t - x^\star\|^3 \\
&= f(x^\star) + \frac{1}{2} \|x_t - x^\star\|_{H_\star}^2 + \frac{\gamma}{6} \|x_t - x^\star\|^3.
\end{aligned}$$

Hence, we have

$$-\frac{1}{2} \|x_t - x^\star\|_{H_\star}^2 \leq -(f(x_t) - f(x^\star)) + \frac{\gamma}{6} \|x_t - x^\star\|^3 \tag{B.3}$$

Therefore, we obtain that

$$\begin{aligned}
& - \|\nabla f(x_t)\|_{\tilde{H}^{-1}}^2 \\
&\leq -\rho \|x_t - x^\star\|_H^2 + \Delta_2 \\
&\leq -\rho \left( \|x_t - x^\star\|_{H_\star}^2 + \langle x_t - x^\star, (H - H^\star)(x_t - x^\star) \rangle \right) + \Delta_2 \\
&\stackrel{(B.3)}{\leq} -2\rho \left( f(x_t) - f(x^\star) - \frac{\gamma}{6} \|x_t - x^\star\|^3 - \frac{1}{2} \langle x_t - x^\star, (H - H^\star)(x_t - x^\star) \rangle \right) + \Delta_2 \\
&\stackrel{(2.4)}{\leq} -2\rho(f(x_t) - f(x^\star)) + \frac{4\gamma\rho}{3} \|x_t - x^\star\|^3 + \Delta_2.
\end{aligned}$$

Now we begin to bound the value of  $\Delta_2$ . First, by the condition  $\nabla^2 f(x) \leq (1 + (1 - \rho))\tilde{H}$ , we



have

$$\begin{aligned}
\|H(x_t - x^*)\|_{\tilde{H}^{-1}} \cdot \|\Delta_1\|_{\tilde{H}^{-1}} &\leq \|x_t - x^*\| \cdot \left\| H\tilde{H}^{-1}H \right\|^{1/2} \cdot \|\Delta_1\| \cdot \left\| \tilde{H}^{-1/2} \right\| \\
&\leq \|x_t - x^*\| \cdot \sqrt{2} \left\| H^{1/2} \right\| \cdot \frac{\gamma}{2} \|x_t - x^*\|^2 \cdot \left\| \tilde{H}^{-1/2} \right\| \\
&\leq \frac{\sqrt{2}\gamma L^{1/2}}{2} \|x_t - x^*\|^3 \cdot \left\| \tilde{H}^{-1/2} \right\|.
\end{aligned}$$

We also have

$$\begin{aligned}
\|\Delta_1\|_{\tilde{H}^{-1}} \cdot \|(H_\star - H)(x_t - x^*)\|_{\tilde{H}^{-1}} &\leq \|\Delta_1\| \cdot \left\| \tilde{H}^{-1/2} \right\| \cdot \gamma \|x_t - x^*\| \cdot \|x_t - x^*\| \left\| \tilde{H}^{-1/2} \right\| \\
&\leq \frac{\gamma^2}{2} \|x_t - x^*\|^4 \cdot \left\| \tilde{H}^{-1} \right\|.
\end{aligned}$$

where the first inequality is because the condition that  $\|H_t - H_\star\| \leq \gamma \|x_t - x^*\|$ . Finally, we have

$$\begin{aligned}
&\|(H_\star - H)(x_t - x^*)\|_{\tilde{H}^{-1}} \cdot \|H(x_t - x^*)\|_{\tilde{H}^{-1}} \\
&\leq \gamma \|x_t - x^*\|^2 \cdot \left\| \tilde{H}^{-1/2} \right\| \cdot \|x_t - x^*\| \cdot \left\| H\tilde{H}^{-1}H \right\|^{1/2} \\
&\leq \sqrt{2}\gamma L^{1/2} \|x_t - x^*\|^3 \cdot \left\| \tilde{H}^{-1/2} \right\|.
\end{aligned}$$

Combining the conditions that  $\|x_t - x^*\| \leq \frac{\rho}{\gamma} \cdot \frac{\tau\zeta^{1/2}}{L^{1/2}}$  and  $\lambda_{\min}(\tilde{H}) \geq \zeta$ , we have

$$\begin{aligned}
\Delta_2 &\leq 3\sqrt{2}\gamma L^{1/2} \|x_t - x^*\|^3 \cdot \left\| \tilde{H}^{-1/2} \right\| + \gamma^2 \|x_t - x^*\|^4 \cdot \left\| \tilde{H}^{-1} \right\| \\
&\leq 5\gamma L^{1/2} \zeta^{-1/2} \|x_t - x^*\|^3 + \frac{\tau}{L} \cdot \rho\gamma L^{1/2} \zeta^{-1/2} \|x_t - x^*\|^3 \\
&\leq 6\gamma L^{1/2} \zeta^{-1/2} \|x_t - x^*\|^3,
\end{aligned} \tag{B.4}$$

where the last inequality is due to  $\tau \leq L$  and  $\rho \leq 1$ . Thus, we get that

$$\begin{aligned}
-\|\nabla f(x_t)\|_{\tilde{H}^{-1}}^2 &\leq -2\rho(f(x_t) - f(x^*)) + \frac{4\gamma\rho}{3} \|x_t - x^*\|^3 + 6\gamma L^{1/2} \zeta^{-1/2} \|x_t - x^*\|^3 \\
&\leq -2\rho(f(x_t) - f(x^*)) + \frac{22}{3} \gamma L^{1/2} \zeta^{-1/2} \|x_t - x^*\|^3,
\end{aligned} \tag{B.5}$$

where the last inequality follows from that  $\rho \leq 1$  and  $\zeta \leq L$ .

Now, we begin to bound the value of term  $\|\nabla f(x_t)\|_{\tilde{H}^{-1}}^3$ . First, we have

$$\begin{aligned}
\|\nabla f(x_t)\|_{\tilde{H}^{-1}}^3 &= \|\nabla f(x_t)\|_{\tilde{H}^{-1}}^2 \cdot \|\nabla f(x_t)\|_{\tilde{H}^{-1}} \\
&\leq \|\nabla f(x_t)\|_{\tilde{H}^{-1}}^2 \cdot \left\| \tilde{H}^{-1/2} \right\| \|\nabla f(x_t)\| \\
&\stackrel{(2.2)}{\leq} L\zeta^{-1/2} \|\nabla f(x_t)\|_{\tilde{H}^{-1}}^2 \cdot \|x_t - x^*\|.
\end{aligned}$$

We can bound the value of  $\|\nabla f(x)\|_{\tilde{H}^{-1}}^2$  as follows:

$$\begin{aligned}
& \|\nabla f(x_t)\|_{\tilde{H}^{-1}}^2 \\
&= \|H(x_t - x^*) + \Delta_1 + (H_\star - H)(x_t - x^*)\|_{\tilde{H}^{-1}}^2 \\
&\leq \|H(x_t - x^*)\|_{\tilde{H}^{-1}}^2 + \|\Delta_1\|_{\tilde{H}^{-1}}^2 + \|(H_\star - H)(x_t - x^*)\|_{\tilde{H}^{-1}}^2 + \Delta_2 \\
&\stackrel{(3.1)}{\leq} \|x_t - x^*\|_H^2 + 2\gamma^2 \left\| \tilde{H}^{-1} \right\| \cdot \|x_t - x^*\|^4 + \Delta_2 \\
&= \|x_t - x^*\|_{H^\star}^2 + \langle x_t - x^*, (H - H^\star)(x_t - x^*) \rangle + 2\gamma^2 \left\| \tilde{H}^{-1} \right\| \cdot \|x_t - x^*\|^4 + \Delta_2 \\
&\stackrel{(2.4)}{\leq} \|x_t - x^*\|_{H^\star}^2 + \gamma \|x_t - x^*\|^3 + 2\gamma^2 \left\| \tilde{H}^{-1} \right\| \cdot \|x_t - x^*\|^4 + \Delta_2 \\
&\leq \|x_t - x^*\|_{H^\star}^2 + 7\gamma L^{1/2} \zeta^{-1/2} \|x_t - x^*\|^3.
\end{aligned}$$

The last inequality is because of Eqn. (B.4),  $1 \leq L^{1/2} \zeta^{-1/2}$  and the condition  $\|x_t - x^*\| \leq \frac{\rho}{\gamma} \cdot \frac{\tau \zeta^{1/2}}{L^{1/2}}$ .

We also have that

$$\begin{aligned}
f(x_t) &\geq f(x^*) + \langle \nabla f(x^*), x_t - x^* \rangle + \frac{1}{2} \langle \nabla^2 f(x^*)(x_t - x^*), x_t - x^* \rangle - \frac{\gamma}{6} \|x_t - x^*\|^3 \\
&= f(x^*) + \frac{1}{2} \|x_t - x^*\|_{H^\star}^2 - \frac{\gamma}{6} \|x_t - x^*\|^3.
\end{aligned}$$

Therefore, we have

$$\begin{aligned}
\|\nabla f(x)\|_{\tilde{H}^{-1}}^3 &\leq L \zeta^{-1/2} \|\nabla f(x_t)\|_{\tilde{H}^{-1}}^2 \cdot \|x_t - x^*\| \\
&\leq L \zeta^{-1/2} \cdot \|x_t - x^*\| \left( 2(f(x_t) - f(x^*)) + \frac{\gamma}{3} \|x_t - x^*\|^3 + 7\gamma L^{1/2} \zeta^{-1/2} \|x_t - x^*\|^3 \right) \\
&\leq 2L \zeta^{-1/2} \|x_t - x^*\| \cdot (f(x_t) - f(x^*)) + 15\gamma L^{3/2} \zeta^{-1} \|x_t - x^*\|^4, \tag{B.6}
\end{aligned}$$

where the last inequality is due to the fact that  $1 \leq L^{1/2} \zeta^{-1/2}$ .

Therefore, we can obtain that

$$\begin{aligned}
& \mathbb{E}_u[f(x_{t+1}) - f(x^*)] \\
&\leq f(x_t) - f(x^*) - \frac{b}{64(d+2)} \|\nabla f(x_t)\|_{\tilde{H}^{-1}}^2 + \frac{b^3 \gamma}{64} d^{-3/2} \left\| \tilde{H}^{-1} \right\|^{3/2} \cdot \|\nabla f(x)\|_{\tilde{H}^{-1}}^3 + \Delta_\mu \\
&\stackrel{(B.5)}{\leq} f(x_t) - f(x^*) - \frac{b\rho}{32(d+2)} (f(x_t) - f(x^*)) + \frac{2b\gamma L^{1/2} \zeta^{-1/2}}{3(d+2)} \|x_t - x^*\|^3 \\
&\quad + \frac{b^3 \gamma}{64} d^{-3/2} \left\| \tilde{H}^{-1} \right\|^{3/2} \cdot \|\nabla f(x)\|_{\tilde{H}^{-1}}^3 + \Delta_\mu \\
&\stackrel{(B.6)}{\leq} \left( 1 - \frac{b\rho}{32(d+2)} \right) (f(x_t) - f(x^*)) + \frac{2b\gamma L^{1/2} \zeta^{-1/2}}{3(d+2)} \|x_t - x^*\|^3 \\
&\quad + \frac{b^3 \gamma L \zeta^{-2}}{64d^{3/2}} \|x_t - x^*\| \cdot (f(x_t) - f(x^*)) + \frac{b^3 \gamma^2 L^{3/2} \zeta^{-5/2}}{4d^{3/2}} \|x_t - x^*\|^4 + \Delta_\mu.
\end{aligned}$$

Since the objective function is  $\tau$ -strongly convex, by Lemma 10, we have

$$\|x_t - x^*\|^3 \leq \frac{2}{\tau} \cdot \|x_t - x^*\| \cdot (f(x_t) - f(x^*)),$$

and by the condition of  $\|x_t - x^*\| \leq \frac{\rho}{\gamma} \cdot \frac{\tau\zeta^{1/2}}{L^{1/2}}$ , we also have

$$\begin{aligned} \frac{b^3\gamma^2 L^{3/2}\zeta^{-5/2}}{4d^{3/2}} \|x_t - x^*\|^4 &\leq \frac{b^3\gamma^2 L^{3/2}\zeta^{-5/2}}{4d^{3/2}} \cdot \frac{2}{\tau} \|x_t - x^*\|^2 \cdot (f(x_t) - f(x^*)) \\ &\leq \frac{b^3\gamma L\zeta^{-2}}{2d^{3/2}} \|x_t - x^*\| \cdot (f(x_t) - f(x^*)). \end{aligned}$$

Thus, we have

$$\begin{aligned} &\mathbb{E}_u [f(x_{x+1}) - f(x^*)] \\ &\leq \left(1 - \frac{b\rho}{32(d+2)}\right) (f(x_t) - f(x^*)) + \frac{4b\gamma L^{1/2}\zeta^{-1/2}}{3\tau(d+2)} \|x_t - x^*\| \cdot (f(x_t) - f(x^*)) \\ &\quad + \left(\frac{b^3\gamma L\zeta^{-2}}{64d^{3/2}} + \frac{b^3\gamma L\zeta^{-2}}{2d^{3/2}}\right) \|x_t - x^*\| \cdot (f(x_t) - f(x^*)) + \Delta_\mu \\ &= \left(1 - \frac{b\rho}{32(d+2)}\right) (f(x_t) - f(x^*)) + b\gamma \cdot \Delta_3 \cdot \|x_t - x^*\| \cdot (f(x_t) - f(x^*)) + \Delta_\mu, \end{aligned}$$

where  $\Delta_3$  is defined as

$$\Delta_3 = \frac{4L^{1/2}\zeta^{-1/2}}{3\tau(d+2)} + \frac{33b^2L\zeta^{-2}}{64d^{3/2}}.$$

To keep a fast convergence rate, we need

$$\begin{aligned} \|x_t - x^*\| &\leq \frac{1}{2\gamma\Delta_3} \frac{\rho}{32(d+2)} \\ &\leq \frac{\rho}{\gamma} \cdot \min\left(\frac{3\tau\zeta^{1/2}}{256L^{1/2}}, \frac{d^{3/2}\zeta^2}{33L(d+2)b^2}\right). \end{aligned}$$

Thus, when  $x_t$  satisfies the above condition, we can obtain that

$$\mathbb{E}_u [f(x_{x+1}) - f(x^*)] \leq \left(1 - \frac{b\rho}{64(d+2)}\right) (f(x_t) - f(x^*)) + \Delta_\mu.$$

□

## B.2 Proof of Theorem 2

Now, we give the global convergence property of Algorithm 1 in Theorem 2.

*Proof of Theorem 2.* Taking a random step from  $x_t$ , we have

$$\begin{aligned}
& \mathbb{E}_u [f(x_{t+1})] \\
&= \mathbb{E}_u \left[ f(x_t - \eta \tilde{H}^{-1} g_\mu(x_t)) \right] \\
&\stackrel{(2.2)}{\leq} \mathbb{E}_u \left[ f(x_t) - \eta \left\langle \nabla f(x_t), \tilde{H}^{-1} \mathbb{E}_u [g_\mu(x_t)] \right\rangle + \frac{\eta^2 L}{2} \mathbb{E}_u \left\| \tilde{H}^{-1} g_\mu(x_t) \right\|^2 \right] \\
&\leq f(x_t) - \eta \|\nabla f(x_t)\|_{\tilde{H}^{-1}}^2 - \eta \left\langle \nabla f(x_t), \tilde{H}^{-1} (\mathbb{E}_u [g_\mu(x_t)] - \nabla f(x_t)) \right\rangle + \frac{\eta^2 L \left\| \tilde{H}^{-1} \right\|}{2} \mathbb{E}_u \|g_\mu(x_t)\|_{\tilde{H}^{-1}}^2 \\
&\leq f(x_t) - \eta \|\nabla f(x_t)\|_{\tilde{H}^{-1}}^2 + \frac{\eta}{2} \left( \|\nabla f(x_t)\|_{\tilde{H}^{-1}}^2 + \|\mathbb{E}_u [g_\mu(x_t)] - \nabla f(x_t)\|_{\tilde{H}^{-1}}^2 \right) \tag{B.7}
\end{aligned}$$

$$\begin{aligned}
& + \frac{\eta^2 L \left\| \tilde{H}^{-1} \right\|}{2} \mathbb{E}_u \|g_\mu(x_t)\|_{\tilde{H}^{-1}}^2 \\
&\leq f(x_t) - \frac{\eta}{2} \|\nabla f(x_t)\|_{\tilde{H}^{-1}}^2 + \frac{\eta \mu^2 L^2}{8} \left\| \tilde{H}^{-1} \right\|^2 (d+3)^3 + \frac{\eta^2 L \left\| \tilde{H}^{-1} \right\|}{2} \mathbb{E}_u \|g_\mu(x_t)\|_{\tilde{H}^{-1}}^2 \tag{B.8}
\end{aligned}$$

$$\begin{aligned}
&\leq f(x_t) - \frac{\eta}{2} \|\nabla f(x_t)\|_{\tilde{H}^{-1}}^2 + \frac{\eta \mu^2 L^2}{8} \left\| \tilde{H}^{-1} \right\|^2 (d+3)^3 \\
& + \frac{\eta^2 L \left\| \tilde{H}^{-1} \right\|}{2b} \left( \frac{\mu^2}{2} L^2 \left\| \tilde{H}^{-1} \right\| (d+6)^3 + 2(d+2) \|\nabla f(x_t)\|_{\tilde{H}^{-1}}^2 \right) \tag{B.9}
\end{aligned}$$

$$\begin{aligned}
&= f(x_t) - \frac{\eta}{2} \|\nabla f(x_t)\|_{\tilde{H}^{-1}}^2 + \eta^2 L (d+2) b^{-1} \left\| \tilde{H}^{-1} \right\| \|\nabla f(x_t)\|_{\tilde{H}^{-1}}^2 \\
& + \frac{\eta \mu^2 L^2}{8} \left\| \tilde{H}^{-1} \right\|^2 (d+3)^3 + \frac{\eta^2 L^3 \mu^2 \left\| \tilde{H}^{-2} \right\|}{4b} (d+6)^3
\end{aligned}$$

Inequality (B.7) is because of Cauchy's inequality and  $2ab \leq a^2 + b^2$ . Inequality (B.8) follows from Lemma 1. and inequality (B.9) is due to Lemma 2 with  $B = \tilde{H}^{-1}$ .

Since  $\zeta I \preceq \tilde{H}$  holds for all iterations, let us set the step size  $\eta$  as

$$\eta = \frac{b\zeta}{4(d+2)L}.$$

Thus we obtain that

$$\mathbb{E}_u [f(x_{t+1})] \leq f(x_t) - \frac{b\zeta}{16(d+2)L} \|\nabla f(x_t)\|_{\tilde{H}^{-1}}^2 + \Delta_\mu,$$

where  $\Delta_\mu$  denotes that

$$\Delta_\mu = \frac{b\mu^2 L}{32(d+2)\zeta} (d+3)^2 + \frac{b\mu^2 L}{64\zeta(d+2)^2} (d+6)^3 = \frac{b\mu^2 L}{32\zeta(d+2)} \left( (d+3)^3 + \frac{(d+6)^3}{2(d+2)} \right).$$

By Lemma 10, we have

$$\begin{aligned}
\mathbb{E}_u [f(x_{t+1}) - f(x^*)] &\leq f(x_t) - f(x^*) - \frac{\zeta}{16(d+2)L^2} \|\nabla f(x_t)\|^2 + \Delta_\mu \\
&\leq f(x_t) - f(x^*) - \frac{\zeta^\tau}{16(d+2)L^2} (f(x_t) - f(x^*)) + \Delta_\mu \\
&= \left(1 - \frac{\zeta}{16(d+2)\kappa L}\right) \cdot (f(x_t) - f(x^*)) + \Delta_\mu
\end{aligned}$$

□

## C Proof of Section 3.4

### C.1 Proof of Theorem 3

Our proof of Theorem 3 relies on the existing results about noisy power method depicted in Algorithm 4. Because of the approximation, we can cast our zeroth-order power method as the noisy power method and the product  $H_\mu V_t$  can be regarded as  $H_\mu V_t = \nabla^2 f(x) V_t + G_t$  with  $G_t$  being the noise matrix. Balcan et al. (2016) showed that the noisy power method converges to the principal eigenvalues and eigenvectors of the matrix and have the follow properties.

**Lemma 11** (Balcan et al. (2016)). *Given positive definite matrix  $H \in \mathbb{R}^{d \times d}$  and  $0 < \epsilon < 1$ , suppose that noise matrix satisfies*

$$\|G_t\| \leq C_1 \epsilon^2 \lambda_{k+1} \quad \text{and} \quad \|V_k^T G_t\|_2 = C_2 \epsilon^2 \lambda_{k+1} \cos(V_k, X_t).$$

Then, after  $T$  iterations,  $V_T$  returned by Algorithm 4 satisfies

$$\|H - V_T V_T^T H\| \leq (1 + \epsilon) \|H - H_k\|, \quad \text{if} \quad T = \frac{C_3}{\epsilon} \log \left( \frac{\tan(U_k, V_0)}{\epsilon} \right).$$

where  $H_k = U_k \Lambda_k U_k^T$  is the best rank- $k$  approximation of  $H$ .  $C_1$ ,  $C_2$ , and  $C_3$  are absolute constants.

*Proof of Theorem 3.* First, we us denote  $H = \nabla^2 f(x)$ . By the definition of  $V_T$  and  $\hat{V}$  in Algorithm 2, we have

$$\begin{aligned}
\|H - V \Lambda V^T\| &\leq \|H - V_T V_T^T H V_T V_T^T\| + \|V_T V_T^T H V_T V_T^T - V \Lambda V^T\| \\
&\leq \|H - V_T V_T^T H\| + \|V_T V_T^T H - V_T V_T^T H V_T V_T^T\| + \|V_T V_T^T H V_T V_T^T - V_T \hat{V} \Lambda \hat{V}^T V_T^T\| \\
&\leq 2 \|H - V_T V_T^T H\| + \|V_T V_T^T H V_T V_T^T - V_T \hat{V} \Lambda \hat{V}^T V_T^T\| \\
&\leq 3 \lambda_{k+1} + \|V_T V_T^T H V_T V_T^T - V_T \hat{V} \Lambda \hat{V}^T V_T^T\|,
\end{aligned}$$

where the last inequality is because of Lemma 11 with  $\epsilon = 1/2$ .

Furthermore, by the step 6 of Algorithm 2, we have

$$\begin{aligned}
\left\| V_T V_T^\top H V_T V_T^\top - V_T \hat{V} \Lambda \hat{V}^\top V_T^\top \right\| &= \left\| V_T^\top H V_T - \hat{V} \Lambda \hat{V}^\top \right\| \\
&= \left\| V_T^\top H V_T - \hat{V} U^\top H_\mu V_T \right\| \\
&\leq \left\| V_T^\top - \hat{V} U^\top \right\| \cdot \|H V_T - H_\mu V_T\| \\
&\leq 2 \|H V_T - H_\mu V_T\|,
\end{aligned}$$

where the last inequality is because of  $\left\| V_T^\top - \hat{V} U^\top \right\| \leq \|V_T\| + \left\| \hat{V} U^\top \right\| \leq 2$ .

Now, we begin to bound the value of  $\|H V_T - H_\mu V_T\|$ . Let  $v$  be a unit vector, we have

$$\begin{aligned}
\left\| \frac{\nabla f(x + \mu_1 \cdot v) - \nabla f(x)}{\mu_1} - \nabla^2 f(x) v \right\| &= \left\| \frac{\nabla f(x + \mu_1 \cdot v) - \nabla f(x) - \mu_1 \nabla^2 f(x) v}{\mu_1} \right\| \\
&= \left\| \frac{\mu_1 \cdot v (\nabla^2 f(\tilde{x}) - \nabla^2 f(x))}{\mu_1} \right\| \\
&\leq \mu_1 \cdot \gamma \|v\|^2 = \gamma \mu_1,
\end{aligned}$$

where the last inequality is because of Eqn. (2.4) and  $\tilde{x} = x + \theta \cdot (\mu_1 v)$  with  $0 \leq \theta \leq 1$ .

Let  $\tilde{\nabla} f(x)$  denote the approximate gradient computed as follows:

$$\tilde{\nabla}_j f(x) = \frac{f(x + \mu_1 \cdot e_j) - f(x - \mu_1 \cdot e_j)}{2\mu_1}.$$

We also use  $\square$  Then, we have

$$\begin{aligned}
&\left\| \nabla f(x) - \tilde{\nabla} f(x) \right\| \\
&= \left\| \left[ \tilde{\nabla}_1 f(x) - \nabla_1 f(x), \dots, \tilde{\nabla}_d f(x) - \nabla_d f(x) \right]^\top \right\| \\
&= \frac{1}{2\mu_1} \cdot \left\| \left[ (f(x + \mu_1 \cdot e_1) - f(x - \mu_1 \cdot e_1) - 2\mu_1 \nabla_j f(x)), \dots, \right. \right. \\
&\quad \left. \left. (f(x + \mu_1 \cdot e_d) - f(x - \mu_1 \cdot e_d) - 2\mu_1 \nabla_d f(x)) \right]^\top \right\| \\
&= \left\| \frac{\mu_1^2 \cdot \text{diag}(\nabla^2 f(\tilde{x}_1) - \nabla^2(\tilde{x}_2))}{4\mu_1} \right\| \\
&\stackrel{(2.4)}{\leq} \frac{\mu_1}{4} \gamma \|\tilde{x}_1 - \tilde{x}_2\| \\
&\leq \frac{\gamma \mu_1^2}{2},
\end{aligned}$$

where the last inequality is because of  $\tilde{x}_1 = x + \theta_1 \cdot (\mu_1 v)$  with  $0 \leq \theta_1 \leq 1$  and  $\tilde{x}_2 = x - \theta_2 \cdot (\mu_1 v)$  with  $0 \leq \theta_2 \leq 1$ .

Combining the above results, we have

$$\begin{aligned}
\|HV_T - H_\mu V_T\| &= \|H[v_1, v_2, \dots, v_k] - H_\mu[v_1, v_2, \dots, v_k]\| \\
&\leq k \|Hv_1 - H_\mu v_1\| \\
&= k \left\| \frac{\tilde{\nabla}f(x + \mu_1 \cdot v) - \tilde{\nabla}f(x)}{\mu_1} - \nabla^2 f(x)v \right\| \\
&\leq k \left\| \frac{\nabla f(x + \mu_1 \cdot v) - \nabla f(x)}{\mu_1} - \nabla^2 f(x)v \right\| \\
&\quad + k \left\| \frac{\tilde{\nabla}f(x + \mu_1 \cdot v) - \nabla f(x + \mu_1 \cdot v) + \nabla f(x) - \tilde{\nabla}f(x)}{\mu_1} \right\| \\
&\leq k \left( \mu_1 \gamma \|v_1\|^2 + 2 \frac{\gamma \mu_1^2}{2\mu_1} \right) \\
&\leq 2k\mu_1\gamma.
\end{aligned}$$

Therefore, we have

$$\|H - V\Lambda V^\top\| \leq 3\lambda_{k+1} + 2\|HV_T - H_\mu V_T\| \leq 5\lambda_{k+1}$$

where the last inequality is because that we set  $\mu$  and  $\mu_1$  as follows

$$k\gamma\mu_1 + 2\sqrt{d}L\frac{\mu}{\mu_1} \leq 2\lambda_{k+1}$$

Furthermore, we can obtain that

$$\begin{aligned}
&\|H - VV^\top H_\mu VV^\top\| \leq 5\lambda_{k+1} \\
&\Rightarrow -5\lambda_{k+1} \|y\|^2 \leq y^\top (H - VV^\top H_\mu VV^\top) y \leq 5\lambda_{k+1} \|y\|^2 \\
&\Rightarrow -10\lambda_{k+1} \|y\|^2 \leq y^\top (H - \tilde{H}) y \leq 0 \\
&\Rightarrow y^\top \tilde{H} y - 6\lambda_{k+1} \|y\|^2 \stackrel{(a)}{\leq} y^\top H y \stackrel{(b)}{\leq} y^\top \tilde{H} y
\end{aligned}$$

Let us consider the  $\stackrel{(a)}{\leq}$  case and have

$$\begin{aligned}
&y^\top \tilde{H} y - 10\lambda_{k+1} \|y\|^2 \leq y^\top H y \\
&\Rightarrow y^\top \tilde{H} y \leq y^\top H y + 10\lambda_{k+1} \|y\|^2 \leq \left(1 + \frac{10\lambda_{k+1}}{\lambda_{\min}}\right) y^\top H y \\
&\Rightarrow \left(1 - \frac{10\lambda_{k+1}}{\lambda_{\min} + 10\lambda_{k+1}}\right) \tilde{H} \preceq H
\end{aligned}$$

---

**Algorithm 4** Noisy Power Method.

---

- 1: **Input:** A positive definite matrix  $H \in \mathbb{R}^{d \times d}$ , orthonormal matrix  $X \in \mathbb{R}^{d \times p}$ , target rank  $k$ ;
  - 2: **for**  $t = 0, \dots$  until termination **do**
  - 3:    $Y_t = HX_t + G_t$  for some noise matrix  $G_t$ ;
  - 4:   QR factorization:  $Y_t = X_{t+1}R_{t+1}$ , where  $V_{t+1}$  consists of orthonormal columns.
  - 5: **end for**
- 

Therefore, we have

$$\left(1 - \frac{10\lambda_{k+1}}{\lambda_{\min} + 10\lambda_{k+1}}\right) \tilde{H} \preceq H \preceq \tilde{H}.$$

□

## C.2 Proof of Theorem 4

*Proof of Theorem 4.* By Theorem 3, it takes  $O(dk \cdot \log(\tan(U_k, V_0)))$  queries to construct the approximate Hessian. We also need  $O(d)$  queries to estimate gradient. By Theorem 1 and 3, we need  $O\left(\frac{d\lambda_{k+1}}{b\tau} \log\left(\frac{1}{\epsilon}\right)\right)$  iterations to achieve an  $\epsilon$ -accuracy. Hence, we have

$$\begin{aligned} Q(\epsilon) &= O\left(\frac{d\lambda_{k+1}}{b\tau} b \log\left(\frac{1}{\epsilon}\right) + \frac{d\lambda_{k+1}}{b\tau} \cdot dk \cdot \tan(U_k, V_0) \log\left(\frac{1}{\epsilon}\right)\right) \\ &= O\left(\frac{dk\lambda_{k+1}}{\tau} \cdot \log(\tan(U_k, V_0)) \cdot \log\left(\frac{1}{\epsilon}\right)\right), \\ &= \tilde{O}\left(\frac{dk\lambda_{k+1}}{\tau} \cdot \log\left(\frac{1}{\epsilon}\right)\right). \end{aligned}$$

□

## D Proof of Section 4

### D.1 Proof of Lemma 4

*Proof of Lemma 4.* By the definition of  $f_\mu(x)$ , we have

$$\begin{aligned} \|\nabla^2 f_\mu(x) - \nabla^2 f(x)\| &= \|\nabla^2 \mathbb{E}[f(x + \mu u)] - \nabla^2 f(x)\| \\ &= \|\mathbb{E}[\nabla^2 f(x + \mu u)] - \nabla^2 f(x)\| \\ &\leq \mathbb{E}[\|\nabla^2 f(x + \mu u) - \nabla^2 f(x)\|] \\ &\leq \gamma \mu \mathbb{E}\|u\| \\ &\leq \gamma \mu (d+1)^{1/2}. \end{aligned}$$

The first inequality is due to Jensen's inequality. The second inequality is by Eqn. (2.4). And the last inequality follows from Lemma 8. □



## D.2 Proof of Lemma 5

*Proof of Lemma 5.* To get a convenient expression, we rewrite Eqn. (2.6) in another form by introducing a new integration variable  $y = x + \mu u$ :

$$f_\mu(x) = \frac{1}{\mu^d M} \int_{\mathbb{R}^d} f(y) \exp\left(-\frac{1}{2\mu^2} \|y - x\|^2\right) dy.$$

Then, its gradient can be written as,

$$\nabla f_\mu(x) = \frac{1}{\mu^{d+2} M} \int_E f(y) \exp\left(-\frac{1}{2\mu^2} \|y - x\|^2\right) (y - x) dy.$$

Then, we have

$$\begin{aligned} \nabla^2 f_\mu(x) &= -\frac{1}{\mu^{d+2} M} \int_E f(y) \exp\left(-\frac{1}{2\mu^2} \|y - x\|^2\right) dy \\ &\quad + \frac{1}{\mu^{d+4} M} \int_E f(y) \exp\left(-\frac{1}{2\mu^2} \|y - x\|^2\right) \cdot (y - x)(y - x)^\top dy \\ &= -\left[\frac{1}{\mu^2 M} \int_E f(x + \mu u) \exp\left(-\frac{1}{2} \|u\|^2\right) du\right] I_d + \frac{1}{\mu^2 M} \int_E f(x + \mu u) u u^\top \exp\left(-\frac{1}{2} \|u\|^2\right) du \\ &= \frac{1}{\mu^2 M} \int_E [f(x + \mu u) - f(x)] u u^\top \exp\left(-\frac{1}{2} \|u\|^2\right) du + \frac{1}{\mu^2} (f(x) - f_\mu(x)) I_d. \end{aligned} \quad (\text{D.1})$$

Furthermore,  $f_\mu(x)$  can also be defined as

$$f_\mu(x) = \frac{1}{M} \int_{\mathbb{R}^d} f(x - \mu u) \exp\left(-\frac{1}{2} \|u\|^2\right) du.$$

Similarly, by introducing  $y = x - \mu u$ , we have

$$f_\mu(x) = -\frac{1}{\mu^d M} \int_{\mathbb{R}^d} f(y) \exp\left(-\frac{1}{2\mu^2} \|y - x\|^2\right) dy.$$

And its gradient is,

$$\nabla f_\mu(x) = -\frac{1}{\mu^{d+2} M} \int_E f(y) \exp\left(-\frac{1}{2\mu^2} \|y - x\|^2\right) (y - x) dy.$$

Then, we have

$$\begin{aligned}
\nabla^2 f_\mu(x) &= \frac{1}{\mu^{d+2}M} \int_E f(y) \exp\left(-\frac{1}{2\mu^2} \|y-x\|^2\right) dy \\
&\quad - \frac{1}{\mu^{d+4}M} \int_E f(y) \exp\left(-\frac{1}{2\mu^2} \|y-x\|^2\right) \cdot (y-x)(y-x)^\top dy \\
&= - \left[ \frac{1}{\mu^2 M} \int_E f(x-\mu u) \exp\left(-\frac{1}{2} \|u\|^2\right) du \right] I + \frac{1}{\mu^2 M} \int_E f(x-\mu u) u u^\top \exp\left(-\frac{1}{2} \|u\|^2\right) du \\
&= \frac{1}{\mu^2 M} \int_E [f(x-\mu u) - f(x)] u u^\top \exp\left(-\frac{1}{2} \|u\|^2\right) du + \frac{1}{\mu^2} (f(x) - f_\mu(x)) I_d. \tag{D.2}
\end{aligned}$$

Combining the Eqn. (D.1) and (D.2), we have

$$\begin{aligned}
\nabla^2 f_\mu(x) &= \frac{1}{2} (\nabla^2 f_\mu(x) + \nabla^2 f_\mu(x)) \\
&= \frac{1}{M} \int_{\mathbb{R}^d} \frac{f(x+\mu u) + f(x-\mu u) - 2f(x)}{2\mu^2} u u^\top \exp\left(-\frac{1}{2} \|u\|^2\right) du + \frac{f(x) - f_\mu(x)}{\mu^2} \cdot I_d.
\end{aligned}$$

Therefore, we have

$$\mathbb{E}_u[\tilde{H}] = \nabla^2 f_\mu(x) + \left( \lambda - \frac{f(x) - f_\mu(x)}{\mu^2} \right) \cdot I_d.$$

The inequality  $\nabla^2 f_\mu(x) \preceq \mathbb{E}_u[\tilde{H}]$  is because of  $f_\mu(x) \geq f(x)$  which is implied by

$$f_\mu(x) = \mathbb{E}[f(x + \mu u)] \geq \mathbb{E}[f(x) + \mu \langle \nabla f(x), u \rangle] = f(x)$$

where the inequality is because of convexity of  $f(x)$ . □

## E Parameter Setting

## F Visualization of Adversarial Attack

Table 3: Parameter settings in MNIST experiments

	Algorithm	$b$	$\mu$	lr	$\nu$
targeted	ZOO	100	0.01	0.5	-
	PGD-NES	100	0.05	0.02	-
	ZOHA-Gauss	100	0.01	0.04	-
	ZOHA-Gauss-DC	50-200	0.01	0.04	-
	ZOHA-Diag	100	0.1	0.04	0.85
	ZOHA-Diag-DC	50-200	0.1	0.04	0.85
un-targeted	ZOO	100	0.01	0.5	-
	PGD-NES	100	0.05	0.02	-
	ZOHA-Gauss	100	0.01	0.04	-
	ZOHA-Gauss-DC	50-200	0.01	0.04	-
	ZOHA-Diag	100	0.1	0.04	0.8
	ZOHA-Diag-DC	50-200	0.1	0.04	0.8

Table 4: Parameter settings in ImageNet experiments

	Algorithm	$b$	$\mu$	lr	$\nu$
targeted	ZOO	50	0.01	2	-
	PGD-NES	50	0.01	0.01	-
	ZOHA-Gauss	50	0.05	0.03	-
	ZOHA-Gauss-DC	50-200	0.05	0.03	-
	ZOHA-Diag	50	0.03	0.015	0.8
	ZOHA-Diag-DC	50-200	0.03	0.015	0.8
un-targeted	ZOO	50	0.01	0.5	-
	PGD-NES	50	0.01	0.01	-
	ZOHA-Gauss	50	0.02	0.02	-
	ZOHA-Gauss-DC	50-200	0.02	0.02	-
	ZOHA-Diag	50	0.03	0.03	0.7
	ZOHA-Diag-DC	50-200	0.03	0.03	0.7

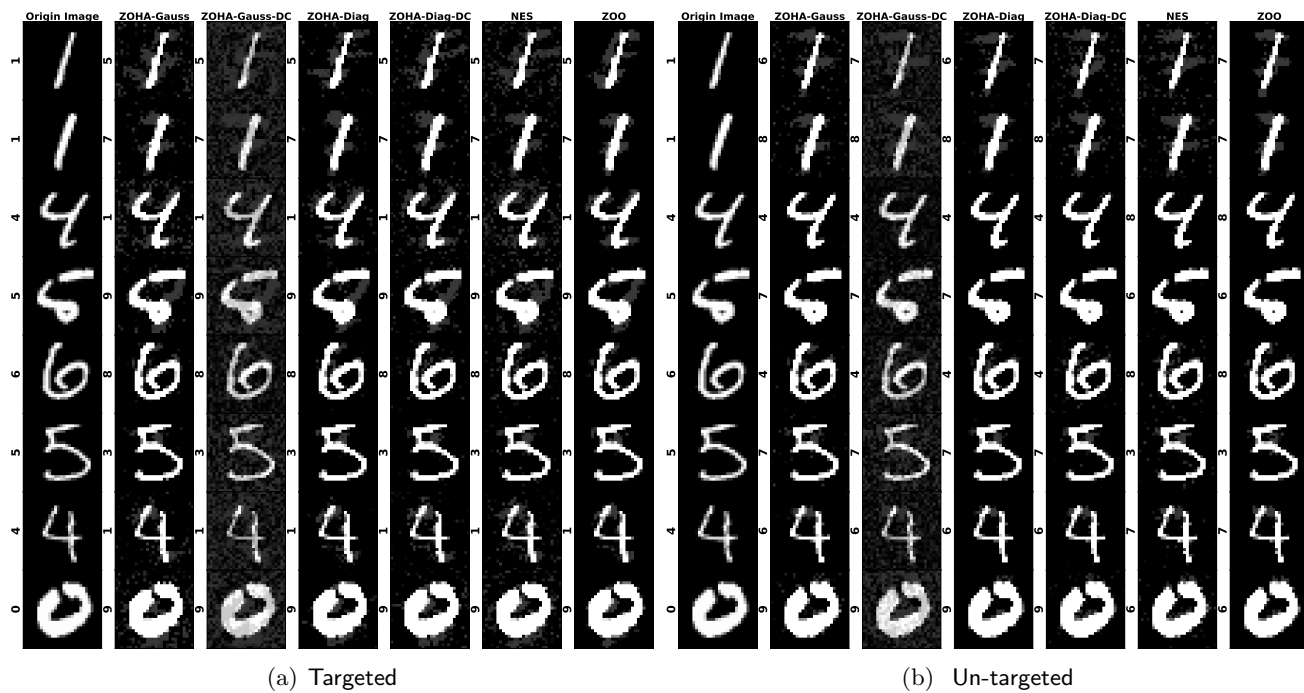


Figure 5: Adversarial examples on MNIST. The label is denoted on the left side.

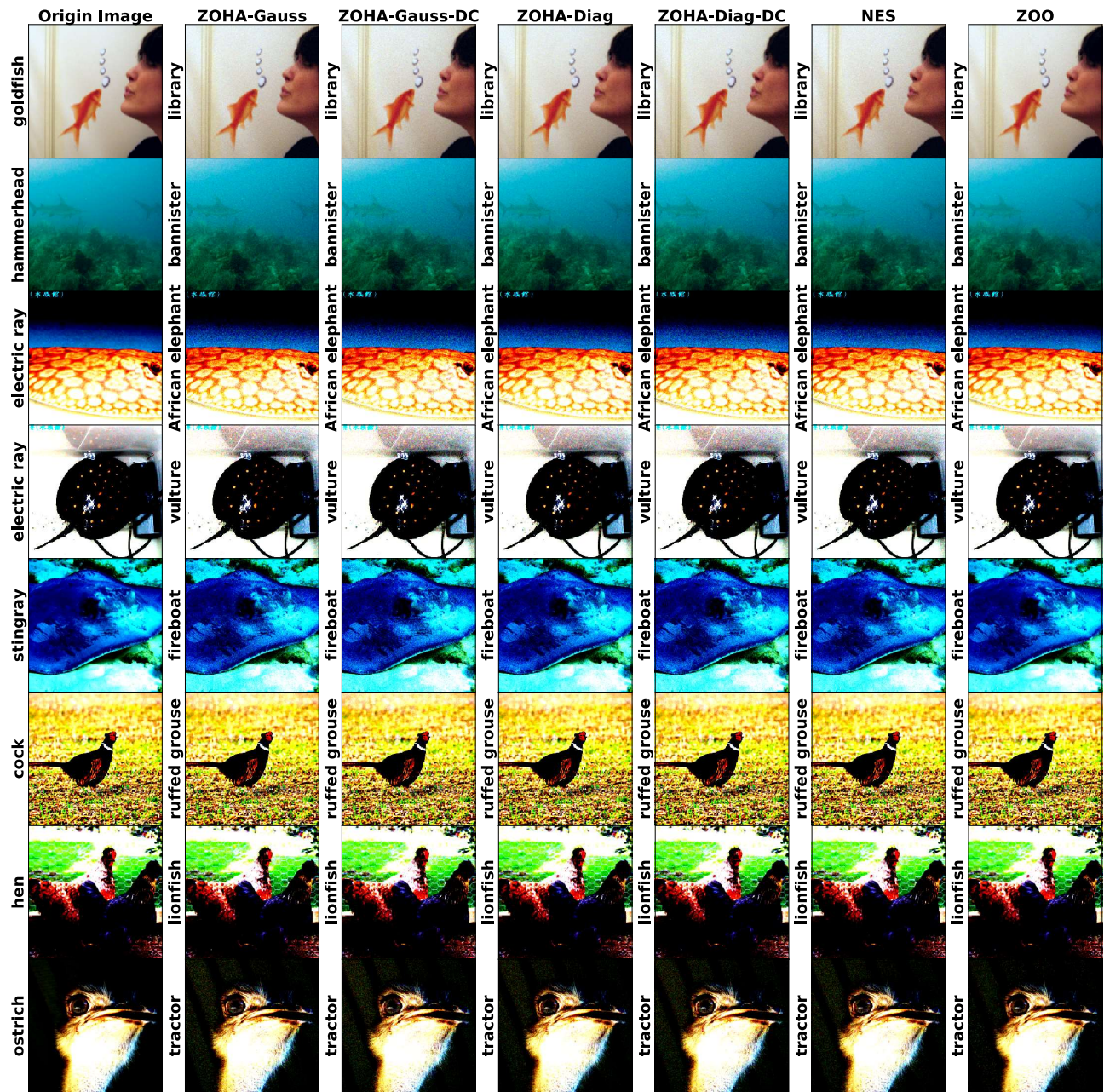


Figure 6: Targeted adversarial examples on ResNet50 and ImageNet. The label is denoted on the left side.

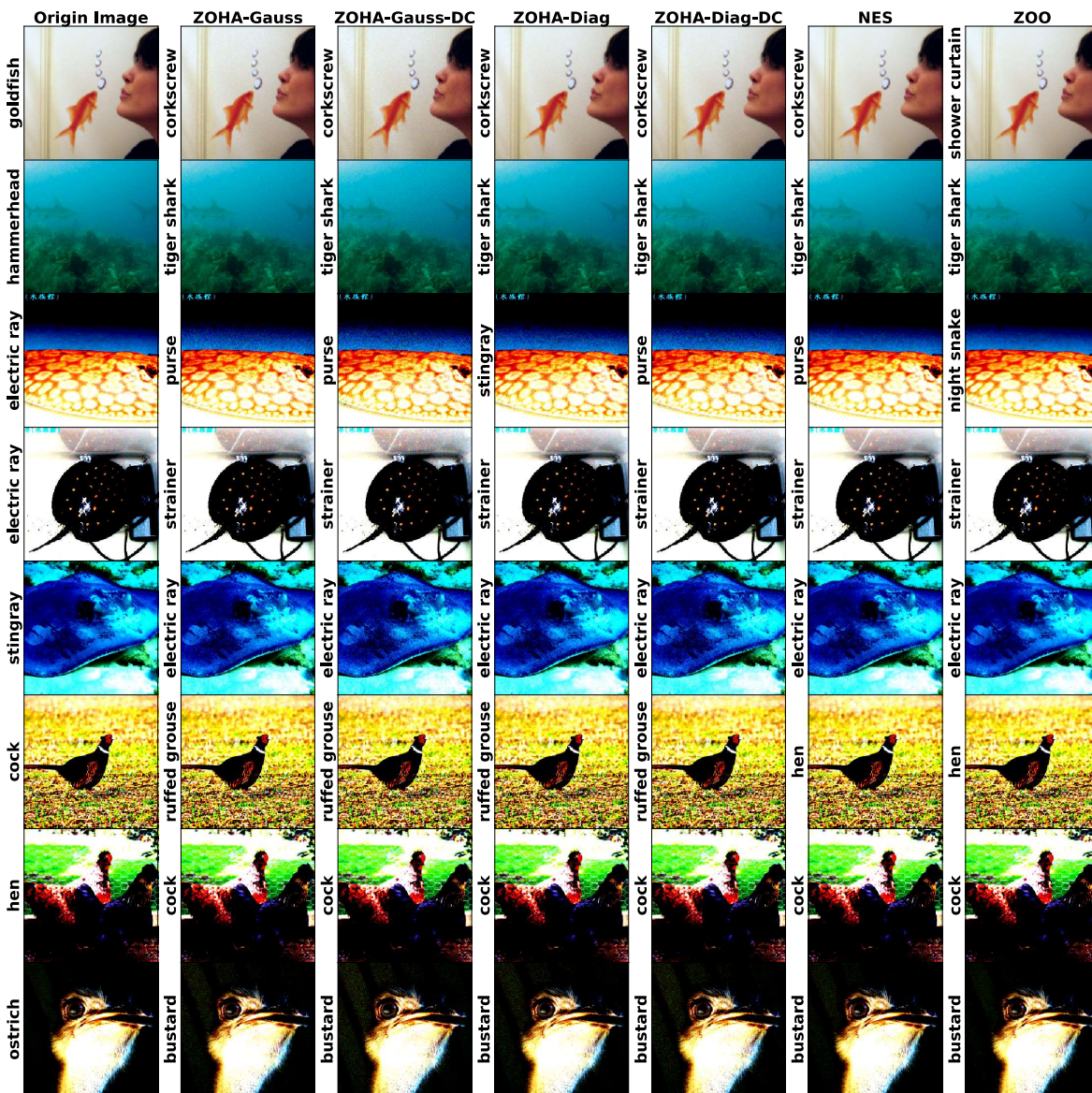


Figure 7: Un-targeted adversarial examples on ResNet50 and ImageNet. The label is denoted on the left side.